Heliyon 10 (2024) e39395

Contents lists available at ScienceDirect

Heliyon

journal homepage: www.cell.com/heliyon

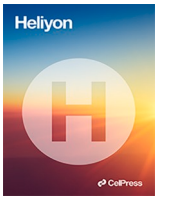

Review article

Functionalized carbon electrocatalysts in energy conversion and storage applications: A review

Yilkal Dessie [a,*], Eneyew Tilahun [a], Tadele Hunde Wondimu [b]

[a] Department of Applied Chemistry, Adama Science and Technology University, Adama, Ethiopia
[b] Department of Materials Science and Engineering, Adama Science and Technology University, Adama, Ethiopia

ARTICLE INFO

Keywords:
Porous activated carbon
Fuel cells
Batteries

ABSTRACT

Energy crises, along with environmental tampering, are currently a big topic on the global scene. The most promising strategy in the current research trend is the creation of ecologically pleasant renewable green alternative energy sources. Since adequate access to green, ecologically acceptable energy sources promotes industrialization and the well-being of human society. Hence, in this review, the most recent carbon electrocatalysts electrode materials prepared from porous activated carbon (PAC) in electrochemical energy conversion and storage systems due to its long life cycle, porosity and high surface area nature as well as low-cost nature have been clearly discussed. This review aims to demonstrate that the increasing interest in the synthesis of PAC is accompanied by extensive research into their application in supercapacitors, where they continue to be the preferred electrode material. Their challenges and current progress of PAC electrodes are also discussed. The systematic methods of modifying PAC from biomass as well as some commercially available carbon materials have been thoroughly summarized in this review as an alternate high-surface area electrode for the effective generation of energy in many energy conversion and storage devices. The critical assessment is also extends to evaluate its recent advancements, trends in research progress, and future prospects.

1. Introduction

In today's civilization, the world economy is expanding quickly, fossil fuel consumption is rising, and natural pollution is getting worse [1]. Hence, storing energy and converting it into a useable form have been considered green and sustainable energy technologies [2,3]. One of the most important problems facing contemporary society is finding pollution-free energy sources to meet the worlds expanding energy needs. It has greatly shifted the focus of research toward the development of more affordable, widely available, and environmentally friendly sustainable sources of energy [4]. In order for human society to develop economically, socially, and politically in a sustainable manner, environmentally friendly energy sources in the form of supercapacitors, fuel cells, and batteries must be provided efficiently by such technologies [5]. Since, direct energy from biomass residues [6] and conventional fuel cells [7] was considered to be an alternative sources of energy to replace fossil and hydrocarbon-based fuel resources. However, both of the energy source are not very sustainable due to their cost-ineffectiveness and environmentally unfavorable nature [8,9].

Research on carbon-based materials in renewable energy technologies have become increasingly important for future renewable energy production and storage applications [10]. In this regard, cost-efective and sustainable high-performance porous carbon

* Corresponding author.
E-mail address: yilikaldessie@gmail.com (Y. Dessie).

https://doi.org/10.1016/j.heliyon.2024.e39395
Received 11 August 2024; Received in revised form 12 October 2024; Accepted 14 October 2024
Available online 15 October 2024

materials from biomass in the form of porous activated carbon (PAC) have been continuously applied for energy storage and conversion roles due to their environmental friendliness nature, due to their dominance of mesoporous diameter range, abundance, and wider surface area with good cycle performance [11,12]. PAC which is prepared by chemical activation followed by integrated pyrolysis (involved with both carbonization and physical activation) have been exploited as an economic and efficient approach toward the production of efficient electrode for renewable energy production and storage applications [13]. Among energy storage systems, supercapacitors are becoming more and more important in the energy storage sector because of their high power density and extended life cycle [14].

Most researchers are focused on preparing abundant, affordable, and environmentally friendly carbon-based electrode materials for converting and storing renewable energy [15]. To enhance energy production of renewable energy using PAC electrodes in many devices, such as fuel cells, batteries, and supercapacitors have received enormous attention today. Due to this, a variety of research have been done to generate such a wonderful, functioning electrode materials from many commercially available carbon compounds [16]. However, the prepared PAC electrodes have demonstrated significant implementation flaws such as excessive cost, poor electrical conductivity, being environmentally unfriendly during preparation and poor cycle stability [17]. Due to this reason, several researchers have been given much attention to biomass based PAC compounds [18]. This is due to the high surface area, porosity, and highly cycle stability nature [19]. As a result, an electrochemical energy storage and conversion technology obtained from biomass is essential for sustainable energy development [20], and the prepared PAC electrode is crucial and cost-effective for the scientific society due to its plentiful, affordable source, environmental friendliness, and practical feasibility.

When PAC is used as anode electrode derived from biomass have a very versatile physicochemical structure and electrochemical properties that makes them ideal for energy storage systems. This criteria is the result of; (i) a high specific surface area (SSA) and hierarchical pore structures with macropores, mesopores, and micropores that can maximize charge/ion storages; (ii) large interlayer spacing that enhance the insertion of cation and anion into the anode microstructure and also offer good mechanical stability for the anodes during the ion insertion/extraction process; (iii) materials with highly active surfaces because of a high number of functional groups on their surfaces, enabling chemical reactions that can enhance the transfer of cation and anion^{-}; and (iv) easily altered by adding other elements that are electrochemically active, such as heteroatoms (N, O, F, H, S, B, etc.), which can enhance its physicochemical properties and subsequently its electrochemical performance [21]. As a result, PAC obtained from biomass can take part in chemical processes or serve as the support for catalysis, and this is said to be an active carbon [22,23]. To increase the performance of the materials like energy storage capacity might be upgraded by using redox additive in aqueous electrolyte. However, such technique is no longer recommendable for commercial level due to using expensive novel transition combination in the form of perovskite materials [24].

2. Biomass and some commercial based PAC materials

The practical applications of PAC generated from biomasses are limited in energy conversion and storage due to their slow electrochemical diffusion kinetics and poor energy storage capabilities [25]. To improve this, researchers have prepared nitrogen and oxygen doped hierarchical PAC composites [26,27]. The potential process to create such biomass-based PAC production for numerous applications is pyrolysis, followed by chemical and physical activations [28,29]. However, it is preferable to employ waste biomass to prepare PAC because commercial procedures for fabricating multidimensional carbon materials via exfoliating graphite oxide tend to be complicated, costly, and inefficient [30].

2.1. Common precursor of PAC materials

PAC materials from diverse biomass sources, such as lignin [31], N-doped carbon [32], and nanosheet [33], carbon from waste plastics, polyethylene terephthalate plastic bottle waste [34], mixed plastic/magnesium oxide [35], laminaria japonica [8], waste straw [36], Water Hyacinth [37], *Borassus flabellifer* flower [38], sorghum-waste [39], were some of them. Most of them exhibited an excellent performance in energy storage devices (i.e., for batteries and supercapacitors) [40]. Because of their superior electrical conductivity, high specific surface area, tunable pore structure, and remarkable physicochemical stability, PAC electrode materials have been extensively employed in supercapacitors [41]. Most of their specific surface areas could be as high as 3839 $m^2\ g^{-1}$ [42]. Recently, in addition to doping with heteroatoms, metal species can also be added with them to further enhance PAC matrix's conductivity and other electrochemical performance without altering the matrix's original structure. In addition to excellent electronic conductivity, the potential for electro-chemical energy storage systems is also greatly influenced by carbon nanomaterials' low cost, easy availability, and ecologically favorable characteristics. Because the N-doped carbon porous materials alter the electronic structure of carbon, they exhibit outstanding electrocatalytic performance, high durability, and large surface area. PAC from biomass is one of the most promising alternatives electrocatalyst to the conventional Pt/C electrocatalysts in many energy conversion and energy storage device applications. The PAC performance greatly increased as a result of the hetero-doping of atoms like N, S, and P with carbon porous materials. This was due to the synergistic interaction of heteroatoms and sp^2 hybridized carbon [43].

It is extended that, majority of biomasses naturally contain nitrogen functionalities, which allow them to self-doped during preparations without the addition of any additives. As a result, majority of PAC generated from biomass are regarded as self-doped carbon materials [44]. Self-doping strategy helps to create an additional defects and active centers with increased electron density and electron-contributing properties. Hence, self-doped PAC electrode materials is highly desirable to increase performance in energy conversion and storage devices [40]. Due to their synergetic features by combining both 2D material structure and porous architectures, their 2D PAC nanosheets with an interlinked hierarchical porous structure have gained a lot of attention in batteries,

supercapacitors, and electrocatalytic oxygen reduction reactions [45]. Additionally, a 3D hierarchical N-doped carbon generated biomass has a rich porous structure, a large specific surface area, and a considerably improved capacity for both mass and electron transport due to this it is effective for a large variety of electroactive species [46]. Furthermore, due to their low-cost, and low environmental pollution nature, biomass carbon materials have been widely used as an effective electrode material in electrochemical double layer capacitors (EDLC). Due to their excellent characteristics for enabling high-performance energy storage, PAC electrodes have the potential to accumulate charges at the electrode/electrolyte interface, especially in EDLC [47].

2.2. PAC electrode supercapacitor performances

For EDLC application, Ghosh et al. [23] have reported cheap, eco-friendly, and easily synthesized PAC electrode materials from banana stem activated by both KOH (KHC) and phosphoric acid (PHC) as well as from corn-cob derived (CHC) and from potato starch derived (SHC) biomasses. Due to improvements in specific surface area and pore size distribution (see Fig. 1(a) and (b)), KOH-activated carbon has among them produced the highest specific capacitance value of 479.23 F g^{-1}. From cyclic voltammetry (CV) probe at high scan rate of 100 mV s^{-1}, the material still maintains its rectangular shape demonstrating that its strong EDLC behavior, as shown in Fig. 1(c). A good supercapacitive behavior is suggested by the charge-discharge (GCD) profile (see Fig. 1(d)), which displays symmetric triangular behavior with low potential (IR) drop. At a current density of 0.5 A g^{-1}, the specific capacitance obtained from GCD curves is 118 F g^{-1}. The electrode material has a lower charge transfer resistance of 4.5 Ω, as shown by the Nyquist curve (Fig. 1(e)). The cycle-ability of KHC electrode material was tested since material cyclic ability is an important factor for real supercapacitor. At a current density of 1 A g^{-1}, the fluctuation of specific capacitance is a function of cycle number (Fig. 1(f)). The electrode material still showed 72.88 % efficiency after 6000 cycles, confirming the good material stability.

In principle, the contact between PAC electrode surface and adsorbed electrolyte layer is where electrical energy is stored in

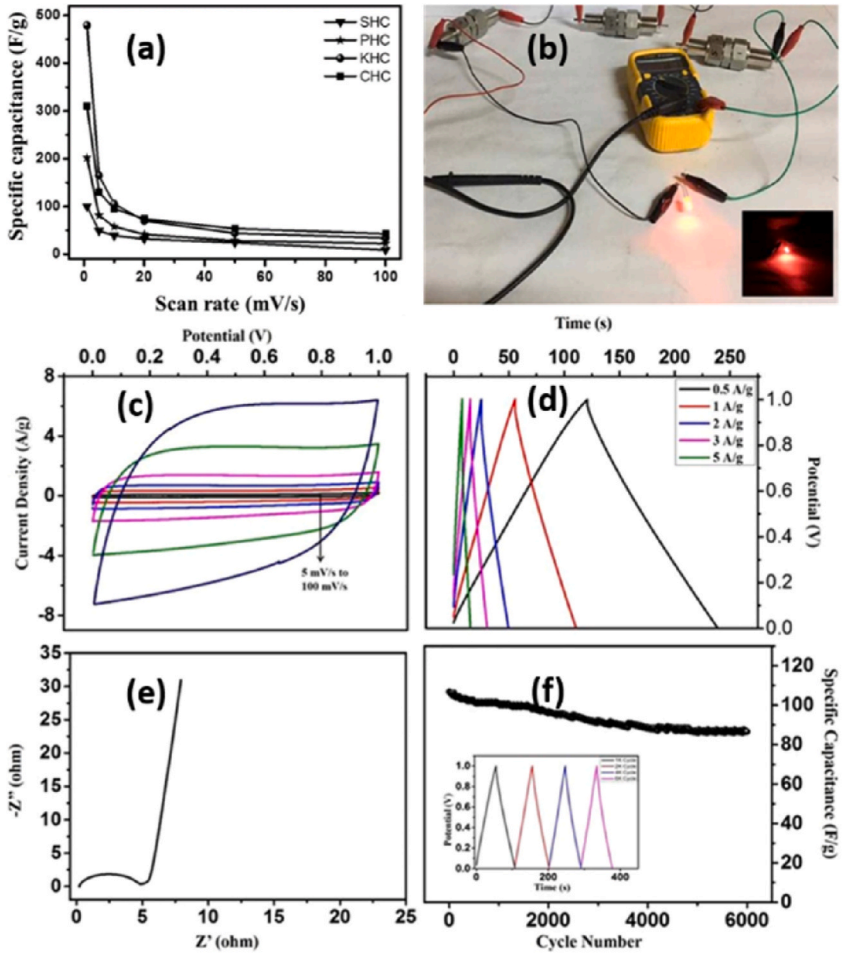

Fig. 1. (a) Specific capacitance vursus scan rates for all prepared carbon. (b) Demonstration of supercapacitor devices prepared by hard carbons. (c) CV of KHC from scan rates 1 mV s^{-1} to 100 mV s^{-1}. (d) GCD curves at different current density in 6 M KOH. (e) Nyquist plot in the frequency range from 0.1 GHz to 0.1 Hz at 5 mV amplitude voltage. (f) Plots of cycle stability over 6000 cycles for KHC. Reproduced with permission from Ref. [23]. Copyright 2019 Springer.

carbon-based supercapacitors. However, due to a slow mass dispersion and limited charge accumulation problem, commercial carbon-based supercapacitors have limited energy densities in organic electrolytes [48]. PAC is primarily distinguished by its large surface area, wide range of pore sizes, relatively low density, and have had their surfaces activated or their structural makeup modified by functionalization or deposition by either metal or metal oxide for specific applications. Pore creation results from surface activation and functionalization, and high-performance supercapacitors heavily rely on these needs [49]. To support this, Zhang et al. [50] have produced hierarchical PAC from low-density polyethylene (LDPE) based materials using KOH as an activating agent. It is intriguing that the non-catalytic carbonization in a closed system yielded 45 % carbon residues from LDPE, although at normal pressure, no other carbon residues would have been produced to manufacture carbon nanomaterials (Fig. 2(a)). A micrometer-sized carbon sphere with a specific surface area of 3059 $m^2\ g^{-1}$ was visible in the acquired PAC. Its charge storage performance was 355 F g^{-1} at a current density of 0.2 A g^{-1} in 6 M KOH electrolyte, as shown in Fig. 2(b). Its energy and power density was found to be 9.81 W h kg^{-1} and 450 W kg^{-1}, respectively, with excellent cycle stability performance. Because of their large specific surface area and superior electrical conductivity, PAC materials with pore channels of various diameters are thought to be promising materials for energy conversion and storage applications [51]. This is due to when a biomass materials are activated either by physical or chemically that enhance predominant of microporous texture with high surface areas [52].

It is crucial that PAC is created using a two-step method that entails both heat carbonization and activation operations [53]. For example, Ananpreechakorn and his co-worker Seetawan [54] have prepared PAC with unique structure made from water hyacinth through thermal followed by chemical activation under argon gas environment. Hence, finally, the performance of the prepared PAC was discovered to exhibit a mixed phase of carbon (90 %) and graphite (10 %). The drying and preparation procedure in detail is illustrated in Fig. 3(a) and (b). It is interesting that, water hyacinth bodies' distinctive microstructure made it ideal for producing huge, porous sheets of carbon, and the detailed methodical preparation step is shown in Fig. 3(c) [54]. Liakos et al. [55] have also prepared PAC from tea-leaf-derived material by following the same procedure, and its estimated surface area was found to be 1151 $m^2\ g^{-1}$ and with a total pore volume between micro and small mesoporous size range. PAC that has larger surface area is desirable for electro-catalyst application due to having its multiple reaction sites [56].

While many efforts have been made to prepare electrode materials with nanostructures and certain chemical compositions in order to increase the performance of electrical energy storage devices, the majority of synthetic methods established have not addressed challenges related to sustainability, cost, or safety. Here, separate tailored strategies are a customized techniques to simultaneously perform the sustainable synthesis, nanostructure engineering, and heteroatom doping of two carbon compounds employing phytic acid and gelatin as biomass precursors. The resulting carbons have homogeneous heteroatom doping and porous nanosheet structures as a result of the customized syntheses. Both of these carbons have been specially used as cathode and anode materials in numerous energy devices due to their usual porosities and chemical compositions [57].

3. Application of PAC and its function in different devices

High surface area, superior electrical conductivity, and high porosity carbon-based materials are recognized as the main substrate for various energy conversion and storage devices, such as fuel cell, supercapacitors, and batteries. The effectiveness of carbon-based materials on the electrocatalytic activity, stability, and output performance of various fuel cells has been studied here [58]. The pore structure of PAC materials can be divided into three categories, namely, micropores (pore size <2 nm), mesopores (2 nm < pore size <50 nm), and macropores (pore size >50 nm) [59]. Based on this information, PAC with a high proportion of ultramicropores (pores less than 1 nm in size) and a suitable mesopore structure provided more charge storage sites. These sites promoted the diffusion of the electrolyte, thereby reducing the internal resistance of the material [60]. Smaller average pore sizes were used to extract higher energy because they enhance the quantity of transferred charges by reducing the ion diffusion distance. As a result, there is a greater chance of ion redistribution, which quickens the rate of voltage increase. Therefore, smaller pore size leads to a higher number of charge transferred and voltage rise [61].

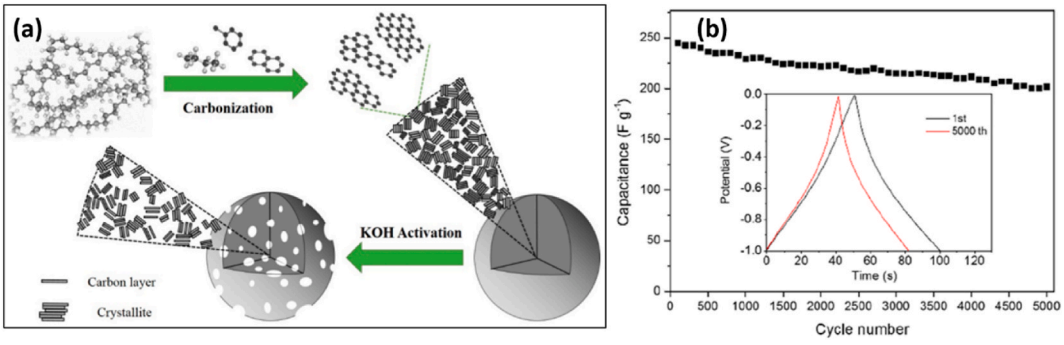

Fig. 2. (a) Schematic diagram of carbonization and LDPE activation using KOH. (b) Cycle stability for HPC-6 at current density of 5 A g^{-1} for 5000 cycles (inset: GCD curve for first and 5000th cycles). Reproduced with permission from Ref. [50]. Copyright 2019 American Chemical Society.

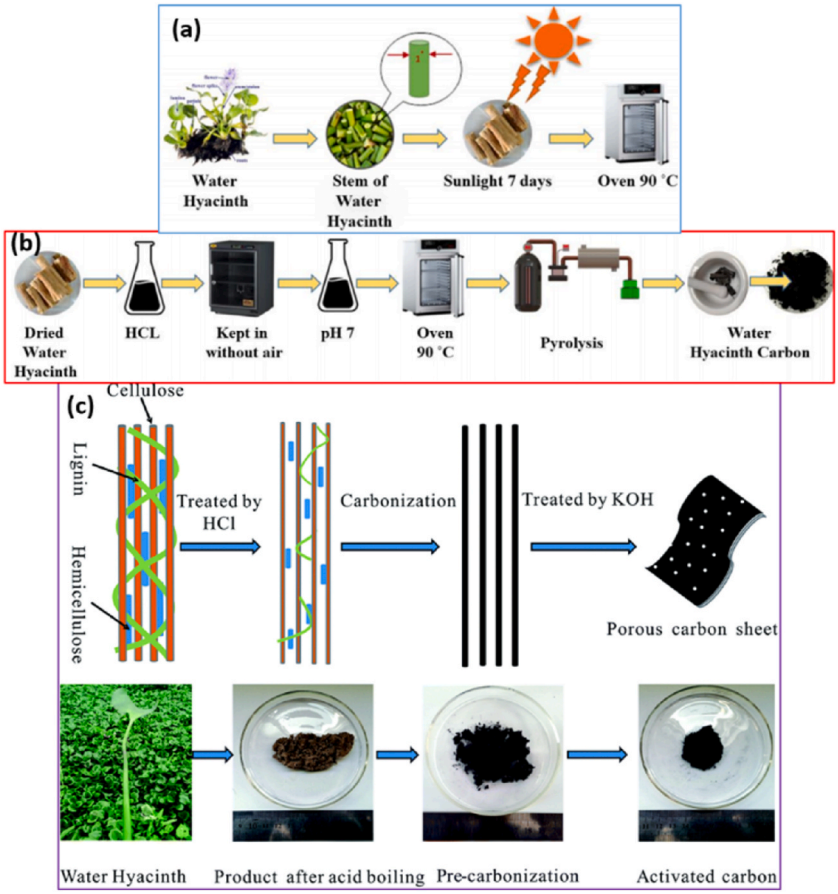

Fig. 3. (a) Schematic diagram for the preparation process of dried and (b) Carbon preparation process. Reproduced with permission from Ref. [54]· Copyright 2021 IOP Publishing. (c) Preparation Water Hyacinth activated carbon preparation process. Reproduced with permission from Ref. [30] Copyright 2016 Royal Society of Chemistry.

3.1. Fuel cell

Similar to batteries, redox reactions are takes place at the two electrodes in contact with an electrolyte in a fuel cell (FC) convert chemical energy into electrical energy [62]. Its efficiency is efficiently increased by the high surface area, high porosity, and electrical conductivity of electrode materials. We have reviewed about the contribution of carbon-based electrode to FC performance and output critically here. As compared to batteries, FC must be recharged after use and can only function as long as fuel is available, FC making them a more appealing option than batteries under open systems [63]. Therefore, FC is an electrochemical current source in which the fuel's chemical energy is directly converted to electrical energy through redox chemical processes. For effective electrodes, a good catalyst support with a large surface area, low resistance, high mechanical strength, and chemical stability is necessary [64]. In FC, an efficient catalyst is necessary for the oxidation of any fuel in order to obtain the necessary current and power densities. For this reason, platinum (Pt) is frequently used as a catalyst in commercially available FC for the oxidation of small organic compounds [65]. However, due to its high cost, Pt is not commercially viable for use in large-scale applications [66]. Thus, researchers have therefore looked for and encountered affordable nanocatalysts from graphene materials in an effort to replace this metal for the efficient generation of electrical powder from the chemical energy [67]. Hence, carbon supports and metal-free carbon materials are among the many materials under investigation that are frequently utilized in FC devices to improve their total electrochemical surface area and performance [58].

Hence, the development of FC applications has been greatly accelerated by graphene and its derivatives. However, the raw material for graphene precursors and the methods of preparation are complex, expensive, nonrenewable and not environmentally benign. It is crucial that most graphene-derived carbon materials, such as carbon nanotubes, have good electrical conductivity, but because of thermal effects, stacking is frequently a problem during the preparation process, and due to the mentioned problem, it is challenging to scale up at the commercial level in FC device systems. To improve this challenge researchers have been integrating graphene with other material. For example, Khantimerov et el [64]. have prepared a nanocatalyst employing pressed porous stainless steel pellets as a substrate to alter expensive carbon nanotubes with less expensive nickel nanoparticles [64]. Instead of preventing electroactive species from entering FC devices, such nanocatalyst structural modifications have improved electronic and ionic transport characteristics [68].

Currently, under the umbrella of carbon materials, compositing carbon with MXene materials is now the current and most popular method for enhancing energy storage and conversion devices [69]. This is because MXenes have alternating layers of carbon and transition metal, giving them with an excellent electrical conductivity (up to 10,000 S cm^{-1}) and allowing for quick electron movement between the electrodes. Therefore, combining carbon materials with MXenes offers new and advanced options in the realm of energy conversion and storage while also resolving all of the most likely problems [70,71]. In such a way, the synthesis, characterization, and application mechanisms of several nanomaterials on microbial and alcohol-based FC have been covered in the following sections.

3.1.1. *Microbial fuel cells*

In the bioelectrochemical technology [72], microbial fuel cells (MFC) [73], have a strong application for electrical energy production in FC system, precious metal recovery, and remediation's of heavy metals from wastewater, followed by the simultaneous treatment of wastewater. Due to the depletion of non-renewable energy resources that contribute negative side effects to environmental damage and the need to produce sustainable energy from accessible renewable sources, MFCs devices have attracted a lot of interest [73,74]. However, the poor bacterial adherence and low extracellular electron transfer (EET) as well as poor anode electrode performance continue to be the main obstacles to the development of MFCs with high power production [75,76]. So, numerous biodegradable organic molecules are the source of electricity that is generated [77,78]. It should be mentioned that the electrode material in MFCs is the most important and impactful part of the MFC device. Additionally, the expenditures associated with cell construction and operation have a detrimental effect on MFC. For example, Offei et al. [79] have prepared an electrode material from palm kernel PAC that is simple, affordable, and effective. It is interesting that this material's novelty, in addition to its affordability and toughness, was also a target. Following testing, the cell produced a maximum voltage and power density of 0.66 V and 1.74 W m^{-3} at 1000 Ω, respectively. As much as 86 % of the value obtained with the widely used bare carbon paper was produced in terms of power density.

In theory, electroactive microorganisms (EAM) were used as a biocatalyst to produce electrons in the anode chamber, and these electrons were then transported by an external circuit to the cathode chamber. EAM to anode and anode to cathode electron transport limitations [80], as well as the slow electron acceptor in the cathode chamber, are the current research challenges that have not been solved yet. To study the anode electrode and electron-accepting species in the cathode chamber, Bian et al. [81] have reported a single-chamber MFCs with an air cathode (carbon cloth (CC) coated with 0.5 mg cm^2 Pt/C) constructed with 3D carbonized anodes in the presence of *shewanella oneidensis* MR-1 biocatalyst. The open porous architectures and inherent biocompatibility of 3D printed porous carbon, which were created using 3D printing anodes, significantly improved the metabolic activities of Shewanella oneidensis MR-1. This prosperity further improved the surface area of anodes since the created 3D roughness was exploited as the perfect foundation for microbial growth and mass transfer. In terms of maximum output voltage, open circuit potential, and power density, the device produced the greatest values of 453.4 ± 6.5 mV, 1256 ± 69.9 mV, and 233.5 ± 11.6 mW m^{-2}, respectively. Under the same conditions, this performance outperformed that of carbon fiber brush anodes and bare CC. Surprisingly, pure natural biomass based PAC is found to be a promising candidate for the rate of substrate oxidation at the anode and oxygen reduction reaction at the cathode [82]. Based on their motivations, Hung et al. [83] have performed a high performance MFC from coffee-waste-derived PAC. Because of its great compatibility with *Escherichia coli* system-based MFCs, the produced PAC proved to be an ideal anode material in the cell

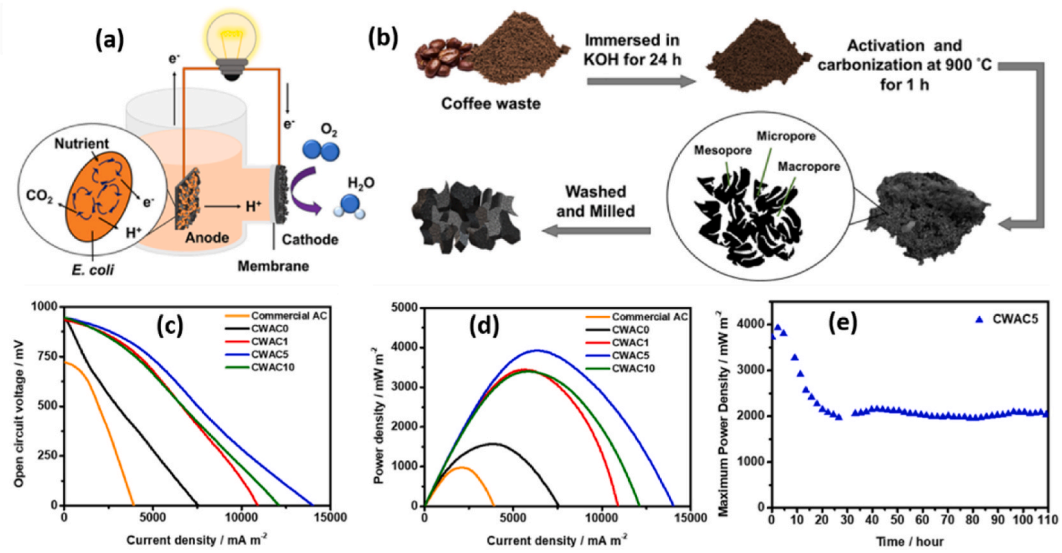

Fig. 4. (a) Schematics of MFC functionality. (b) Coffee-waste-derived activated carbons synthesis. (c) Polarization curves. (d) Power densities. (e) Power density profiles of coffee waste to KOH at a ratio of 1:0, 1:1, 1:5 and 1:10. Reproduced with permission from Ref. [83]. Copyright 2019 American Chemical Society.

designs. Due to pore size modification of AC, it achieved a high maximum power density with a values of 3927 mW m^{-2}, which is bigger in efficiency than commercial AC with 975 mW m^{-2} of power density. The MFCs schematic diagram, AC synthesis, and measured parameters (Fig. 4(a–e)).

Modification of anode electrode with carbon material has continued to increase MFC performance. Kalathil et al. [84] have modified the anode of electrode with carbon nanotube and MnO_2 nanocomposites. Thus, with an external resistance of 800 Ω and an open circuit voltage (OCV) of 1.07 ± 0.02 V, the composite modified anode displayed a maximum power density of 120 ± 1.7 mW m^{-2}, while the corresponding current density was 0.262 ± 0.015 A m^{-2}. OCV is a crucial marker for the high charge density that the bioanode's nanomodifier's charge accumulation causes to form on the bioanode. To reduce the cost of anode electrodes prepared from commercially available carbon nanotubes and their derivatives, Li et al. [85] have discovered a high-performance MFC electrode material made from porous carbon obtained from almond shells that is affordable (Fig. 5(a–d)). shows PAC was created by activating $ZnCl_2$ under N_2 at 800 °C. The PAC as-derived has shown strong conductivity, a large surface area, a linked, hierarchical porous structure, and good biocompatibility. It had a surface area of 616.04 m^2 g^{-1}, a pore volume of 0.51 cm^3 g^{-1}, and an average pore size of 9.68 nm. The anode can provide a maximum power density of 4346 mW m^{-2}, which is significantly greater than that of the MFCs with corresponding carbon and the commercial CC as the MFC anode (Fig. 5(e–h)). With a value of 2059 mW m^{-2}, the power density produced by porous carbon after $ZnCl_2$ activation was greater than that of a reduced graphene oxide/polyaniline/platinum (rGO/-PANI/Pt) composite modified anode [86].

Due to the improved physicochemical and electrochemical properties, self-nitrogen-doped PAC nanosheet modified anode materials will be able to improve MFC performance. Hence, Xing et al. [87] have reported porous carbon made from dandelion seeds by activating the self-doped nitrogen porous carbon nanosheets both with and without KOH. The SEM images of CC were arranged neatly, and the surface was smooth (Fig. 6(a)). A large amount of self-doped AC nanosheet (N-CNS) was loaded on the surface of self-doped PAC nanosheet-CC (N-CNS-CC) carbon fiber and formed a rough surface with more pore structure (Fig. 6(b)), while the self-doped unactivated carbon nanosheet (N-UA-CNS) had fewer pores than N-CNS, and had a lot of carbon particles rather than nanosheet layers (Fig. 6(c)). So, the BET surface area of N-CNS was 2107.5 m^2 g^{-1}, which was much higher than that of N-UA-CNS. After carbon clothes were modified by the obtained materials, the internal resistance of both N-CNS-modified CC (N-CNS-CC) and N-UA-CN-S-modified CC (N-UA-CNS-CC) was greatly reduced and found to be only 2.7 Ω and 4.0 Ω, respectively, which are all significantly smaller than that of blank CC (65.1 Ω) (Fig. 6(d)). The N-CNS modification greatly enhanced maximum output voltage, significantly improved output stability, and decreased start-up time after electrodes were assembled in MFCs as the anode, according to operation trials (Fig. 6(e)). The CC-, N-CNS, and N-UA-CNS-CC-anode MFCs had maximum power densities of 689.13 mW m^{-2}, 1122.41 mW m^{-2}, and 878.92 mW m^{-2}, respectively, and their corresponding current densities, at which maximum power densities were attained, were 2.08 A m^{-2}, 3.06 A m^{-2}, and 2.34 A m^{-2}, respectively, (Fig. 6(f)). This is due to the increasing growth sites for EAM on porous

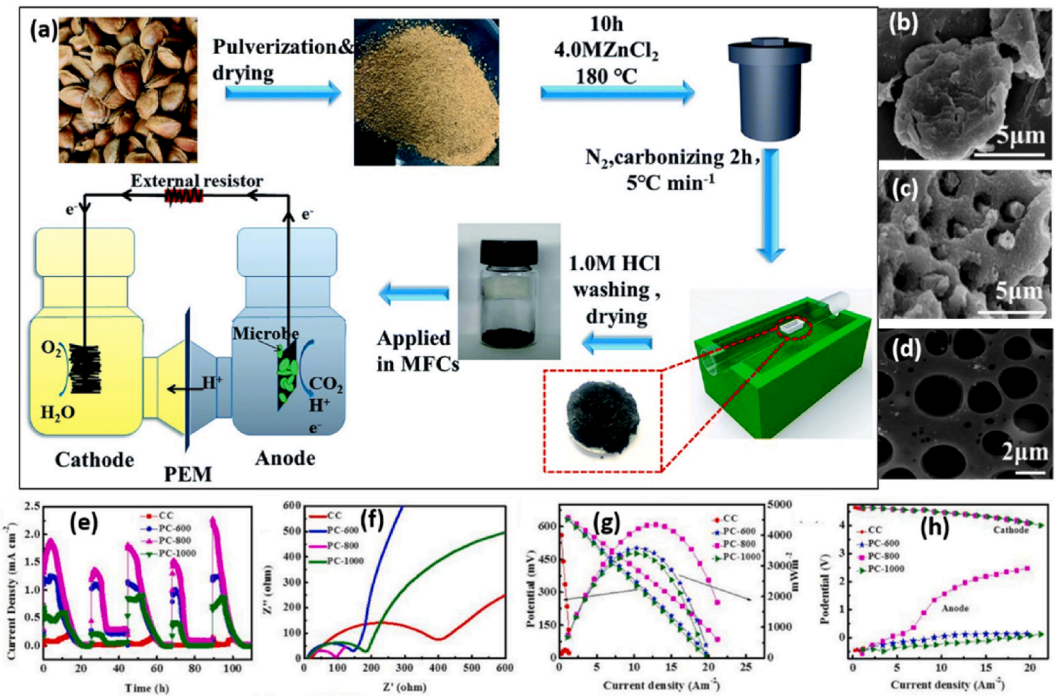

Fig. 5. (a) Schematic diagram for porous carbon production from almond shell and the MFCs. (b) SEM image of untreated almond shell. (c) SEM image of treated carbon at 800 °C. (d) TEM image for treated carbon at 800 °C. (e) Current density vs. time. (f) Nyquist curves for different carbon anodes during MFCs test. (g) Both polarization and power density curve vs. current density. (h) Both anode and cathode polarization curves with different carbon anodes calcined at different temperature. Reproduced with permission from Ref. [85]. Copyright 2019 Royal Society of Chemistry.

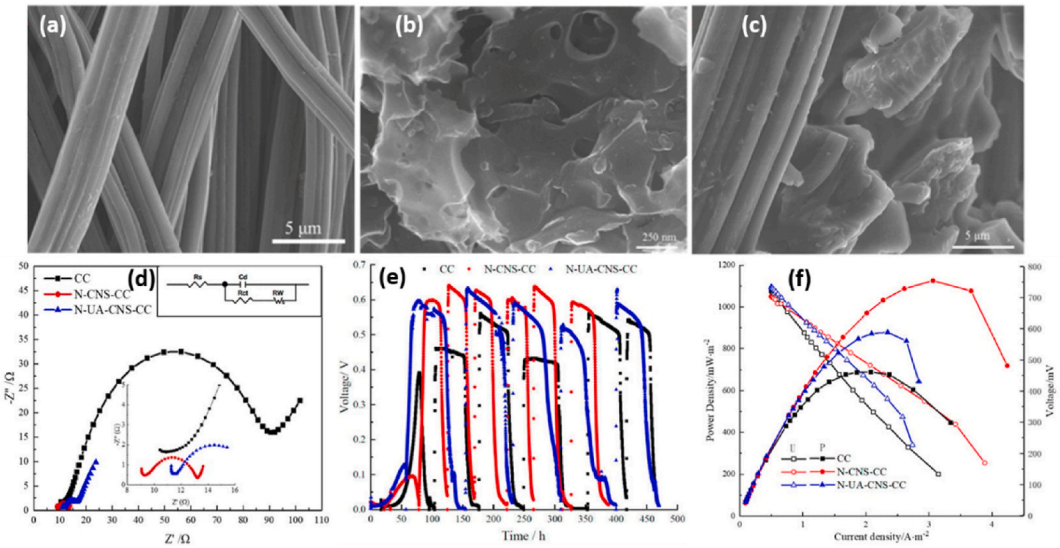

Fig. 6. (a) SEM images for CC. (b) N-CNS-CC. (c) N-UA-CNS-CC. (d) Nyquist plots. (e) Voltage outputs. (f) Polarization and power density vs. current density curves for CC, N-CNS-CC, and N-UA-CNS-CC anodes. Reproduced with permission from Ref. [87]. Copyright 2020 MDPI.

surface features, as revealed by the SEM image. Additionally, CC's conductivity and hydrophilicity were also improved by nitrogen doping [87].

In addition to the involvement of PAC along with the anode, the PAC cathode electrode is a further limiting element for MFC, and it mostly influences the efficiency of the device due to the subpar kinetics of oxygen reduction reaction in the medium. To improve this,

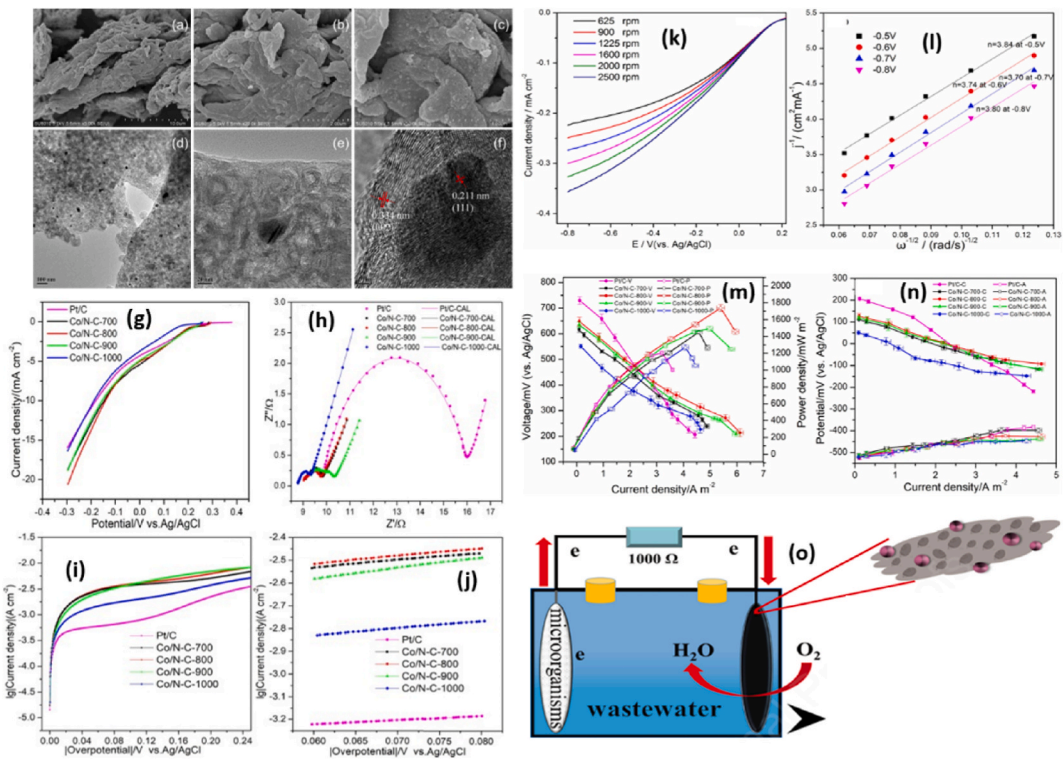

Fig. 7. (a, b, and c) SEM images of Co/N-C-800. (d, e, and f) TEM images of Co/N-C-800. (g) LSVs of different cathodes. (h) Nyquist plots of EIS of different cathodes. (i) Tafel plots of different cathodes. (j) Linear fitting of overpotential from 60 to 80 Mv. (k) RDE voltammograms of Co/N-C-800. (l) Koutecky-Levich plot at different potentials. (m) Polarization and power density curves. (n) Individual polarization curves of cathodes and anodes potential. (o) MFC setup. Reproduced with permission from Ref. [89]. Copyright 2019 Elsevier.

Ghasemi et al. [88] have changed cathodes using carbon black doped by nickel nanoparticles (Ni/C), copper phthalocyanine and carbon black (CuPc/C), and phthalocyanine/carbon (Pc/C). The outcomes demonstrated that Ni/C and CuPc/C were two possible substitute catalysts for Pt. The power produced by CuPc/C was almost as close to Pt. The ORR features of electrodes changed by CuPc/C have the greatest peak and a greater positive potential elucidated from cyclic voltammogram and linear sweep voltammetry (LSV) data. Because of its larger catalytic surface area than other electrodes, this catalyst greatly facilitates ORR. Consequently, utilizing CuPc/C cathode, the maximum power density and coulombic efficiency (CEs) were attained to be 118.2 mW m^{-2} and 29.3 %, respectively. Liang et al. [89] have also reported a high-performance cobalt (Co) nanoparticle cathode from chitosan. Co has been prepared utilizing a one-step high-temperature calcining technique at 700, 800, 900, and 1000 °C, and is embedded in a porous carbon cathode catalyst to increase oxygen reduction reaction. The removal of superfluous Co NPs, which uniformly emerged throughout the surface of the carbon matrix, resulted in the formation of tiny round, pore-like, and wrinkled pictures (Fig. 7(a–c)). Co nanoparticles are visible (Fig. 7(d–f)), which is a TEM picture, and they are embedded in the carbon layer. The sample treated at 800 °C showed a larger current density at −0.3 V than the other catalysts indicating that it had stronger oxygen reduction reaction activity (Fig. 7(g)). The rate of electron transfer associated with the ORR can be inferred from the electrochemical impedance spectroscopy (EIS) spectra acquired at OCV and fitted in a Nyquist plot. The total resistances (R_t) of Co/N-C-800 were reduced, with values of 9.584 Ω, according to the fitting results (Fig. 7(h)). Due to its low electron transfer resistance (fast in oxygen reduction reaction) and high exchange current density, Co/N-C-800 treated at 800 °C exhibits high electrocatalytic activity (Fig. 7(i) and (j)). The limiting current density rose with increasing disk rotational speed in the rotating disk electrode (RDE) test, which was used to further confirm the process of electron transfer. The electron transfer number of Co/N-C-800 was 3.70–3.84 (close to 4), as surveyed from 0.5 V to 0.8 V, manifesting a four-electron transfer process for the ORR (Fig. 7(k) and (l)). Hence, the maximum power density of Co/N-C-800 is 1738 ± 40 mW m^{-2}, which is 44.5 % higher than that of Pt/C (1203 ± 18 mW m^{-2}) (Fig. 7(m) and (n)). This is caused by porous carbon's small average pore size of 3.72 nm and high specific surface area of 335.08 m^2 g^{-1}. The existence of these qualities might offer sufficient oxygen and expose active areas that support the oxygen reduction reaction. With the aid of Co nanoparticles and graphitic-N, the high specific area with the largest total pore volume (0.31 cm^3 g^{-1}) was able to improve the oxygen transport channels at the cathode of MFC (Fig. 7(o)) [89]. Excellent power output and a greater treatment rate were achieved by the MFC stack due to the unique combination of highly PAC particles deposited onto the conductive network of carbon fibers, which simultaneously boosted electrocatalytic activity and increased surface area [90]. So, in general the maximum power density and other respective parameters in MFCs are summarized in Table 1.

3.1.2. Alcohol fuel cells

Alcohol fuel cells produce electricity directly from the electrooxidation of alcohols, which can be thought of as an alternative to fossil fuels, and help to achieve the most pressing climate challenges, including carbon neutrality. Under this cells, the direct alcohol fuel cells (DAFCs) are gaining interest as environmentally friendly and efficient energy conversion devices. Alcohols are simpler to handle and store than conventional hydrogen-fed polymer based electrolyte membrane FC and have a higher volumetric energy density [63]. Thus, alcohol fuel cell-based energy sources from methanol and ethanol, represented as direct methanol fuel cells (DMFC) and direct ethanol fuel cells (DEFC), respectively, have attracted much attention in an effort to replace hydrogen-based fuels due to the

Table 1
Summary of material type, synthesis method, electrode type and power density from different PAC materials in MFCs.

Material source	Synthesis method	Specific surface area (m^2 g^{-1})	Anode	Cathode	Power density (mW m^{-2})	References
Soybeans	Carbonization at 900 °C for 2 h	651.78	Graphite felt	N-doped PAC	977 ± 32	[91]
Ground nutshells (GAC)	Pyrolysis at 600 °C for 2 h	476.83	CC	GAC-modified CC	521	[92]
Coffee waste	Carbonization at 900 °C for 1 h	428	coffee waste-derived AC/CC	commercial AC/CC	3927	[83]
Silver grass (SG)	Carbonization at 600 °C for 1 h	3027	SGAC/CC	plain CC	963 mW cm^{-2}	[93]
Lotus leaves	Carbonization at 900 °C for 2 h	908.90	graphite plate	Lotus leaves AC	511.5 ± 25.6	[94]
Mango wood	Carbonization at 1050 °C for 2 h	–	Mango wood AC	Pt/C	589.8	[95]
Corncob seed	Carbonization at 1000 °C for 3 h	–	Corncob seed AC	Pt/C	1963.1	[96]
Mango seed	Carbonization at 1100 °C for 3 h	–	Mango seed AC	Pt/C	2171	[97]
Sugarcane refuse (SR)	Carbonization at 500 °C for 1 h	–	CC	Sugarcane refuse PAC/ stainless steel mesh	110 ± 6.58	[98]
Coconut shell (CS)	Carbonization at 600 °C for 1 h	–	CS/Cu	Cu	47.04 ± 0.5	[99]
Lignin powder	Carbonization at 1100 °C	225.007	GO/TiO_2/graphite rod	graphite rod	0.57	[100]

CC = carbon cloth, GO = Graphene Oxide,.

disadvantages that mainly relate to transportation and storage related to their safety aspects [7].

The polarization and power density curves for the air-breathing, laminar flow-based, MFCs operating in both acidic and alkaline media under the same operating circumstances provide support for the comments made (see Fig. 8(a) and (b)). According to the curves, laminar flow DMFCs operating in alkaline media performed better than operating in acidic media. Operation in acidic and alkaline mediums was found to have a maximum power density of 11.8 and 17.2 mW cm^{-2}, respectively [101]. So, to study further in alkaline media, Morales S et al. [102] have made an electrocatalyst for oxygen reduction reaction in 0.5 M KOH from the leaves, stem, and roots of water hyacinth. The AC from stem that was calcined at 730 °C (WH_SA730) and activated by KOH had the best pore size distribution, mesoporous and microporous structure, and a high surface area of 1969 m^2 g^{-1}, which was supported by the results. Because of its high surface area and high nitrogen content, the PAC had good electrochemical activity (the potential for oxygen reduction reaction was measured using WH_SA730 at 0.9 V), but other samples' oxygen reduction reaction potentials were created at lower reduction potentials because of their weak catalytic activity. For a better understanding, the performance efficiency of ethanol- and methanol-based FC is briefly described in the sections that follow.

3.1.2.1. Methanol fuel cell. DMFC has proven to be a highly promising power source in a variety of portable electronic devices like cell phones, laptop computers, battery charges etc [103]. However, the high price of membrane electrode assembly limits its practical applications. Due to an increase in electrocatalytic surface active area and a reduction in the necessary loading, Pt particles are frequently spread onto a high surface area conductive substrate, typically carbon black or carbon powder [104,105]. But for commercialization of the cell, obviously Pt is not cost-effective, and hence evaluation of the cell by using cost-effective PAC substrates as catalyst supports for the cathode is a very crucial direction [68], and modifying the anode with a ruthenium (Rt) hybrid with Pt to minimize the poisoning of released gases [106]. Commercially available carbon materials were also chemically activated using KOH to create an alternate electrode, even to improve the performance of carbon materials and substitute Pt in DAFCs. Hence, Perugupalli et al. [107] have looked at the performance of such an electrode in DMFCs and the cell performance was improved by 64 % with a raise of 320 % in maximum power density after treatment with KOH. Sarapuu et al. [108] have also reported a heteroatom-doped carbon modified transition metal electrode based FC device system using alkaline membrane for electrocatalysis of oxygen reduction reaction. According to the cell device mechanism, anion exchange membrane-DMFCs consume water at the cathode rather than creating it (see Fig. 9(a) and (b)). However, both the oxygen reduction reaction and methanol oxidation are kinetically faster in an alkaline state than in an acidic one (Fig. 9(c)).

$$\text{Anode}: CH_3OH + 6OH^- \rightarrow CO_2 + 5H_2O + 6e^- \quad E_o = -0.81\ \text{V} \tag{1}$$

$$\text{Cathode}: \frac{3}{2}O_2 + 3H_2O + 6e^- \rightarrow 6OH^- \quad E_o = 0.40\ \text{V} \tag{2}$$

$$\text{Overall}: CH_3OH + \frac{3}{2}O_2 \rightarrow CO_2 + 2H_2O \quad E_o = 1.21\ \text{V} \tag{3}$$

3.1.2.2. Ethanol fuel cells. In this type of FC, ethanol is used as a fuel instead of the more toxic methanol and has some unique futures. Ethanol is a hydrogen-rich liquid, and it has a higher specific energy (8.0 kW h kg^{-1}) compared to methanol (6.1 kW h kg^{-1}). Ethanol can be obtained in great quantity from various agricultural biomass sources through the fermentation process, and using ethanol could overcome the storage and infrastructure challenges of hydrogen for FC applications. Therefore, due to the stated reason, DEFC has direct application performance in micro portable electronic devices [65]. Ethanol is the best solvent for creating catalyst ink in electrochemistry that produces with a maximum power density of 27.07 mW cm^{-2} in proton and anion exchange membrane DEFCs [109]. Li et al. [110] presented two types of 20 % Pd/C on carbon-support DEFC catalysts. $NaBH_4$ and NaH_2PO_2 reductants were used in the impregnation reduction technique to create the catalyst. The catalysts are totally reduced, as shown by XRD and TEM analyses,

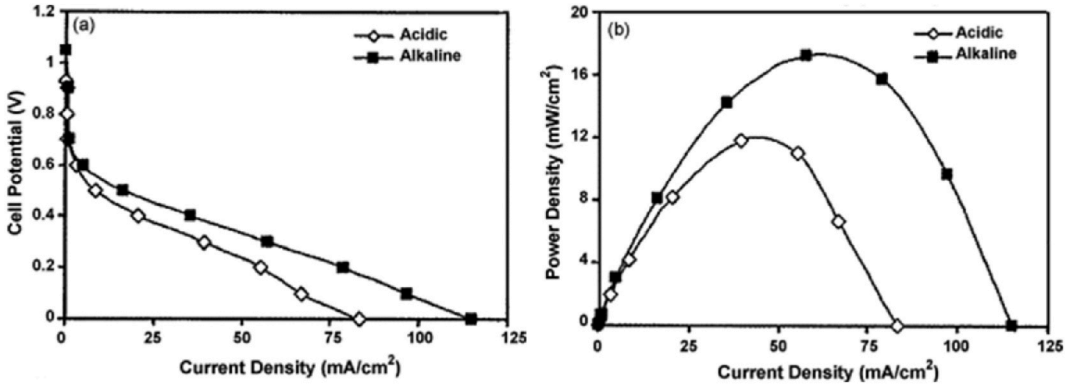

Fig. 8. (a) Polarization curve. (b) Power density curves for an air-breathing, direct-methanol air-breathing laminar flow-based direct methanol fuel cells operated in either alkaline or acidic media at room temperature. Reproduced with permission from Ref. [101]. Copyright 2009 Elsevier.

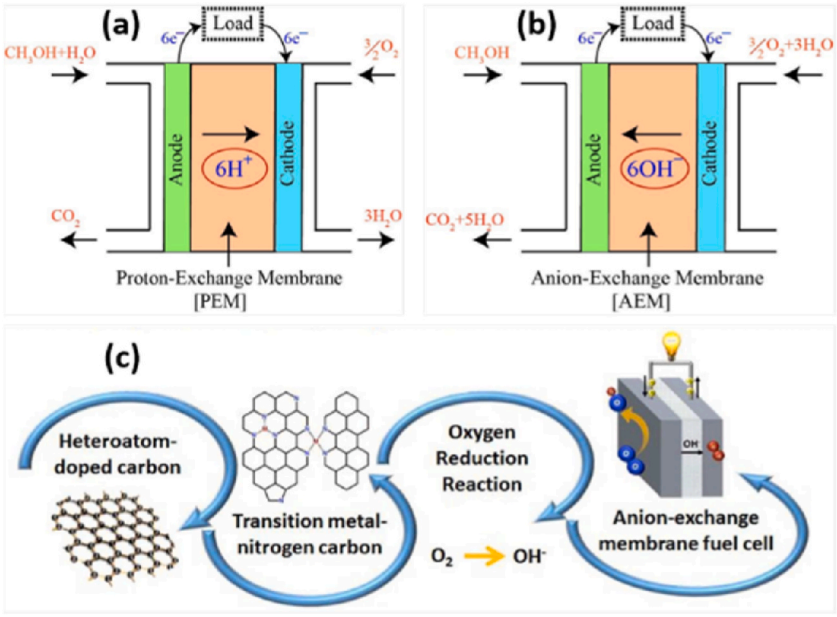

Fig. 9. (a) Schematic of PEM compared. (b) AEM-DMFC. (c) Schematic illustration of AEMFC performance using non-precious metal cathode catalysts. Reproduced with permission from Ref. [108]. Copyright 2018 Royal Society Chemistry.

and they are spherical and uniformly spread over carbon. The results showed that the average particle size of catalysts was 3.3 nm (see Fig. 10(a–c)). CV tests show that the E_{onset} on Pd/C ($NaBH_4$) was more negative than Pd/C (NaH_2PO_2); and showed better catalytic performance, when $NaBH_4$ was used as the reducing agent (Fig. 10(d)). The peak current densities of Pd/C ($NaBH_4$) (28.8 mA cm^{-2}) are higher than Pd/C (NaH_2PO_2) (17.4 mA cm^{-2}). After a 3600 s chronoamperometry test at −0.3 V, Pd/C ($NaBH_4$) exhibits a better stable electrocatalytic activity towards the ethanol oxidation reaction in the alkaline media than Pd/C (NaH_2PO_2) (Fig. 10(e) and (f)). The main reason is that $NaBH_4$ exhibits a higher reduction rate; it is beneficial to maintain a high saturation degree during the nucleation stage at the beginning of the reaction. As a result, the electrochemical activity of Pd/C ($NaBH_4$) was much higher than that of Pd/C (NaH_2PO_2) due to the better electrochemical active surface area of Pd/C ($NaBH_4$) with a value of 56.4 m^2 g^{-1}.

In general, different treatment techniques, such as thermal treatment, potassium hydroxide (KOH) treatment, N_2 doping, and reaction-area control via a multi-layered structure were investigated to increase the reactivity of PAC for alkaline alcoholic fuel cells. This strategy has an advantage to comprehend the distinct electrochemical behaviors of the treated carbon electrodes and determine the most effective way to improve cell performance [107].

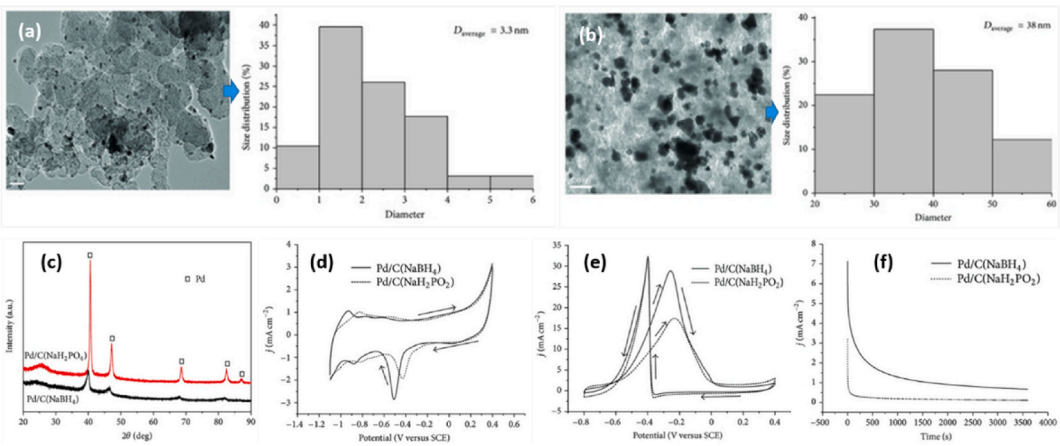

Fig. 10. (a) TEM images and its particles size distribution for Pd/C ($NaBH_4$). (b) TEM images and particle size distribution for Pd/C (NaH_2PO_2). (c) XRD patterns. (d) CV curves in 1 M KOH. (e) CV curves in 1 M C_2H_5OH + 1 M KOH. (f) Chronoamperometry curves in 1 M C_2H_5OH + 1 M KOH solution at a fixed potential of −300 mV for 3600 s. Reproduced with permission from Ref. [110]. Copyright 2013 Hindawi.

3.1.3. Oxygen reduction reaction

Oxygen reduction reaction (ORR) is clearly known that for clean energy conversion technologies, such as clean hydrogen production, ORR has received a lot of attention in FC system due to simultaneously reduce traditional fossil fuel usage and greenhouse gas emissions. Although Pt metal is currently utilized as an electrocatalyst to speed up slow ORR kinetics. However, its high-cost and limited supply still prevent its usage in large-scale applications. Due to their adaptable physico-chemical characteristics and affordable precursors, carbon electrocatalysts generated from biomass have been widely used for ORR electrocatalysis [111]. Hence, Liu et al. [112] have produced a nitrogen-self-doped PAC-based electrode made from water hyacinth. The electrode was extremely comparable to commercial 20 % Pt/C catalysts in terms of ORR efficiency and metal-free catalyst composition in alkaline media. The created self-doped PAC displayed a BET surface area of up to 950.6 $m^2\ g^{-1}$, and it was discovered that different types of nitrogen (pyridinic, pyrrolic, and graphitic) were incorporated into the structure of the carbon molecule [112]. Sun et al. [113] have also created a bifunctional, nitrogen self-doped, metal-free PAC (N-PAC) electrocatalyst with good characteristics (see Fig. 11(a)). The materials had a high specific surface area (1300.58 $m^2\ g^{-1}$) and improved ORR across the board for all pH levels. Additionally, the TEM picture revealed that the sample had an irregular and porous structure with an average pore diameter of 22 nm, as shown in Fig. 11(b). In addition to that, the high-resolution TEM images showed that the N-PAC/800 had a nanosheet structure similar to graphene (see Fig. 11(c)). With an initial potential of 0.92 V for N-PAC/800 in alkaline media, which is close to the commercial Pt/C catalyst (0.93 V), the ORR polarization curves demonstrate that a non-zero cathode current of all the samples arises when the electrode is scanned negatively (Fig. 11(d)). The performance of NC/800's hydrogen evolution reaction (HER) is so excellent, and the potential corresponding to the onset current is 0.855 V (Fig. 11(e)). In terms of PAC samples, it can be seen that all of the samples perform significantly better in HER than N-C/800. In general, ORR is the main parameter indicater for both fuel cells and metal-air batteries. However, this could be more effective when the electrodes composed from metals like platinum. But platinum and other precious metals are not cost-effective and poor in stability, researchers today are focused on hetroatome doped PAC materials [114].

3.2. Battery

In order to address the future energy shortage, the energy research community is particularly interested in electrochemical energy storage systems. Since the electrodes are essential parts of these devices, using effective electrode materials becomes essential. Carbon materials are among the most desirable electrode materials for batteries, because of their plentiful supply, low-cost, excellent stability, nontoxicity, and high level of safety. When these carbon compounds are used as electrode materials, they may be readily obtained from biomass, which improves battery performance [115]. So, to deliver this, extensive attempts have been made to utilize biomass-derived carbon materials as energy storage materials in high-energy rechargeable batteries, particularly due to the sustainability, environmental friendliness, and structural diversity of these materials [116]. In recent years, biomass waste products have shown promise as effective precursors for the manufacture of hard carbon-based anodes in batteries [117]. This is due to the porous network structure that connects amorphous carbon molecules [118]. On the other hand, it is well known that graphene and its derivatives make

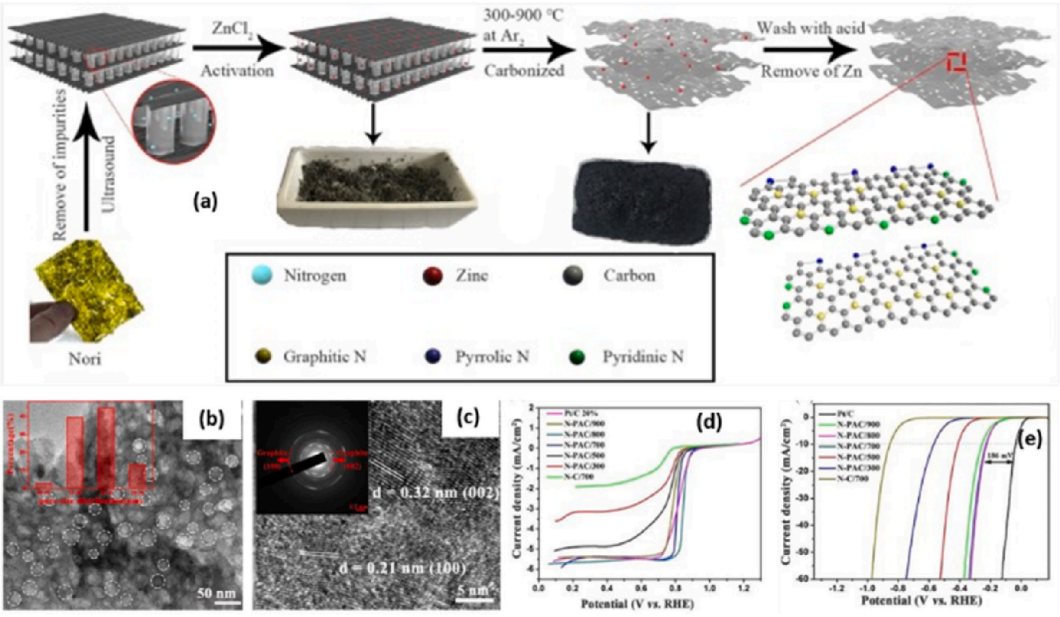

Fig. 11. (a) Schematic diagram for the synthesis process for N-PAC at different activation temperature. (b) TEM (inset is pore diameter distribution). (c) High-resolution TEM image and SAED pattern (inset) of N-PAC/800. (d) ORR polarization curves of different samples in O_2-saturated 0.1 M KOH with a scan rate of 10 mV s^{-1} at 1600 rpm. (e) LSV curves of different samples in 0.5 M H_2SO_4 for HER. Reproduced with permission from Ref. [113]. Copyright 2020 Elsevier.

promising candidates for energy storage due to their huge specific surface area and strong electric conductivity [119]. Particularly, its anode function in lithium ion (Li^+)-based batteries has an excellent electrochemical performance. Its widespread applicability has been painfully constrained by the extreme restacking of graphene brought on by the π-π interaction between neighboring carbon layers. The construction of 3D-structured flakes is required to prevent the restacking of carbon layers in order to fully provide the specific capacity of graphene and expand the area that is accessible to ions [120]. Therefore, in this review, the electrochemical performances of various PAC materials and their modifications with other supportive materials are briefly discussed by listing various secondary rechargeable batteries, such as lithium-ion, sodium-ion, lithium-sulfur, aluminum-air, zinc-air, and lithium-oxygen, batteries.

3.2.1. *Lithium-ion*

Lithium-ion (Li^+) is the most popular energy storage system [121], and has been commercialized to meet the sustained market's demands in computers, electronic devices, and electric vehicles. Today, in comparison to traditional Li^+ cells, the anode-free lithium cell architecture offers exceptional advantages in terms of both energy density and safety thanks to its fully lithiated cathode and bare anode current collector. However, the small Li reservoir (usually zero lithium excess) in the cell architecture makes it difficult to achieve high Li reversibility [122], Thus, to overcome such challenges, researchers have extensively researched and focused on biomass-derived PAC electrocatalysts as efficient and sustainable anode candidates for Li^+ [123]. Functionally, its cell contains anode and cathode electrodes, where anode provides the electron capacity and the cathode delivers electron power density [124]. The electric double-layer and highly porous electrodes with a large surface area are used in Li^+ battery design enabled to reduce the gap between the opposing charges and boost capacitance. Um et al. [125] have tried to generate a very micropore PAC by physically activating porous, rich coffee-derived biomass using only steam. In Li^+ batteries, the developed materials served as a reliable reversible anode electrode. After 100 cycles, the produced electrode demonstrated with an excellent cycle stability and a reversible capacity of ~200 mA h g^{-1} (i.e., 0.54 lithium per 6 carbons) at a current density of 100 mA g^{-1}, suggesting that the bulk diffusion of lithium is advantageous in the absence of any conducting agent [125]. Additionally, an electrode for Li^+ batteries made from chicken feather biomass active carbon has been produced after activating with KOH followed by heat activation at temperature changes of 750, 850, and 950 °C. Due to the difference in the microstructure of the materials, the activation procedure had a substantial impact on their electrochemical characteristics. Due to its greater interlayer spacing, substantial surface area, strong electronic conductivity, and ion rise, the PAC pyrolyzed at 850 °C exhibits a maximum discharge capacity of 285.78 mA h g^{-1}, good cycling stability, and rate performance. As a result, the battery performance was greatly enhanced by the existence of such features [126].

Due to the limited physical activation capability, which results in the low surface structure of the active site, its capacity is still too

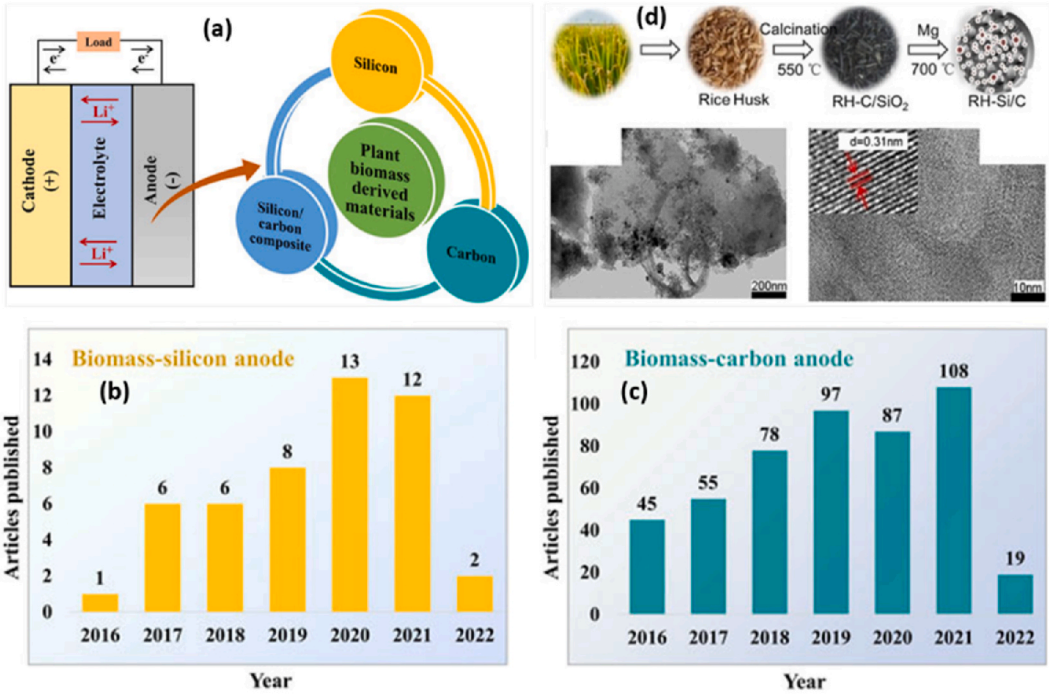

Fig. 12. (a) Plant biomass-derived Si, carbon, and Si/C composite used as anode materials for Li^+ batteries; publication status on biomass-derived materials for Li+ from 2016 to March 2022. (b) Biomass-silicon anodes. (c) Carbon biomass anode. Biomass silicon and biomass carbon anode data status from Web of Science from site searching. Data from Web of Science by searching "biomass silicon anode" or "biomass carbon anode" and "Li^+ battery". (d) Schematic diagram for the preparation of Si/C composite from rice husk (RH) via calcination and magnesiothermic reduction method, TEM image of RH-derived carbon (at 200 nm), TEM images of RH-derived Si/C composite (at 10 nm). Reproduced with permission from Ref. [132]. Copyright 2022 Frontiers.

low. Therefore, chemical activation plays a more advanced role than physical activation in filling the gap [127]. Due to this reason, Guan et al. [128] have revealed a hemp stem-derived nanoporous carbon that was produced using a low-temperature carbonization with a high-temperature activation approach. Because of the benefits of the naturally porous structure of the hemp stem, the findings of the characterizations revealed that PAC had larger pores. The prepared PAC has mesopores and macropores, as well as a mostly microporous aperture size. When the prepared PAC was used as an anode in Li^+ battery, it offers a good reversible capacity with a values of 495 mA h g^{-1} after 100 cycles at a temperature of 0.2 °C. The appropriate pore size distribution and enhanced specific surface areas of the PAC, which reach 589.54 m^2 g^{-1}, greatly improve the property compared to the graphite electrode. Hence, the anode is recognized as a potential device to store high charge in battery [128]. To improve the size of porous carbon further, Yu et al. [129] have used pyrolysis and hydrothermal activation to convert sisal fibers into amorphous carbon anode materials. The generated PAC had a size in the 2–5 nm range and performed well during cycling in Li^+ batteries. Graphite carbon is also utilized as the anode in commercial Li^+ because of its great cycle stability and high electrical conductivity, which provide a theoretical capacity of 372 mA h g^{-1}. Typically, graphite is extracted from the ground or synthetically produced using petroleum coke as a feedstock, both of which are unfriendly to the environment. It is therefore essential and not economical at the commercial level. On the other hand, a current collector graphite foam that is widely employed in electrochemical energy conversion and storage systems is made using graphite as a precursor material [130]. Thus, graphite foams can be utilized in place of existing alloys to create lighter lead acid batteries since they have high electrical and thermal conductivities, good mechanical strength, and low bulk [131].

Therefore, due to their advantageous features, carbon compounds generated from biomass have recently begun to garner significant interest as anode materials for Li^+. New anode materials with greater capacity were required for advanced Li^+ to meet the demand for renewable energy. Since silicon (Si), a naturally generated biomass, has a low working potential (0.4 V vs. Li/Li^+) and a large theoretical specific capacity (3579 mA h g^{-1}), it is the material of choice for the next-generation of Li^+. The Si anode's electrodes are crushed during the lithiation-delithiation process due to the large volume change (300 %), which is a significant disadvantage. The cost-effective alternative anode candidate for Li^+ to replace the commonly used graphite has thus been developed by combining Si with PAC from biogenic silica (SiO_2) and diverse biomass sources, as shown in Fig. 12(a) and (d). It is claimed that the rise in publications over the past several years reflects the growing interest in using Si and electrocatalytically active carbon produced from biomass as anodes in Li^+ (see Fig. 12(b) and (c)) [132].

By enhancing the kinetics of Li^+ diffusion and reducing the stress placed on the graphite matrix by Li^+ intercalation, graphite with

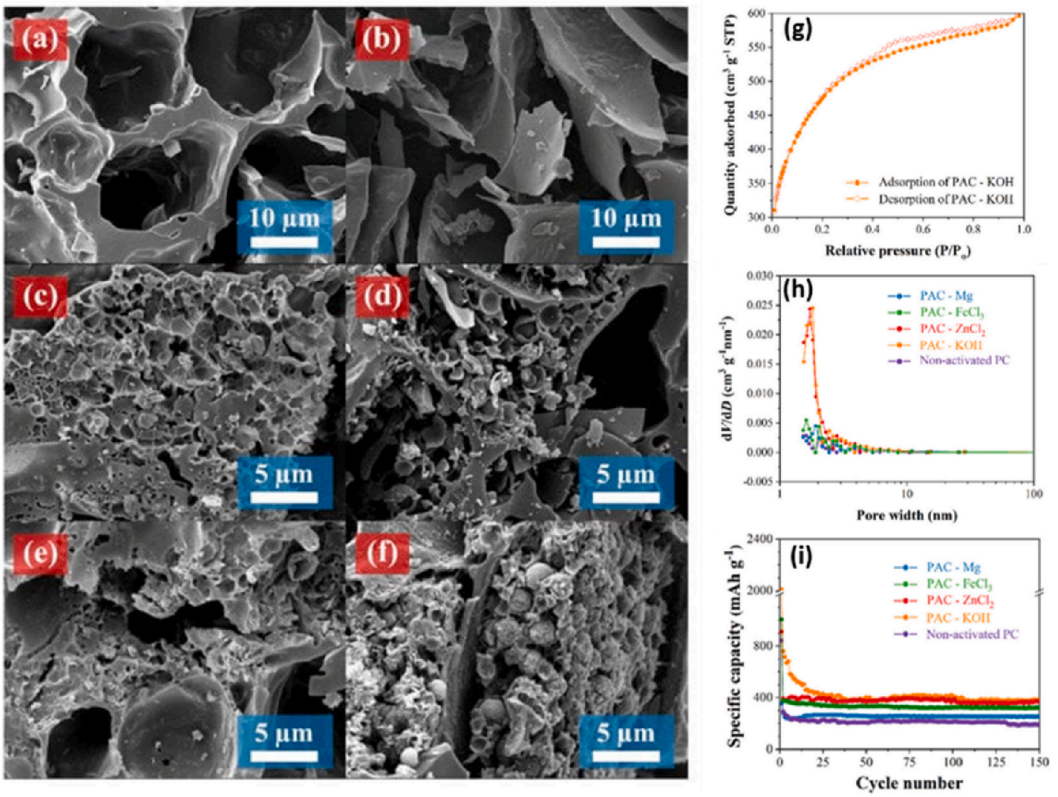

Fig. 13. (a and b) SEM images of non-activated PC. (c, d, e, and f) SEM images of PAC samples with different activating agents, such as KOH, $ZnCl_2$, $FeCl_3$, and Mg, respectively. (g) N_2 adsorption-desorption isotherm of KOH. (h) Pore size distribution of all samples calculated with the BJH model. (i) Cycle performance of all measurements of all prepared electrodes as anode materials for Li^+ battery at 100 mA g^{-1}. Reproduced with permission from Ref. [118]. Copyright 2022 MDPA.

high porosity and wider interlayer spacing may be able to meet the fast-charging requirement. To show this, Thapaliya et al. [133] have prepared a low-cost biomass-derived highly crystalline nano-graphite through a low-temperature electrochemical graphitization method at 850 °C. The resulting graphite exhibits high purity, crystallinity, a high degree of graphitization, and a nanoflake architecture that all ensure fast lithium diffusion kinetics (~2.0 × 10^{-8} cm^2 s^{-1}) through its nanosheet. Such unique features enable outstanding electrochemical performance (~200 mA h g^{-1} at 5C for 1000 cycles, 1C = 372 mA g^{-1}) as a fast-charging anode for Li^+ batteries [133]. However, an anode made from waste avocado seeds beats graphene in terms of both stability and capacity in Li^+ batteries, produces with good cycle stability over 100 cycles and with an equivalent capacity to graphite with a value close to 315 mA h g^{-1} at a current density of 100 mA g^{-1}. This criteria allows the waste biomass based PAC anode to overcome the low diffusion coefficient of 4.38 x 10^{-11} cm^2 s^{-1} [134]. Disordered carbons generated from biomass are continually and effectively used as an alternate anode in Li^+ batteries due to the constrained diffusion coefficients. Hence, Hernández-Rentero et al. [121] have made an alternative anode from cherry pit biomass. To improve the specific surface area and permit porosity, PAC was chemically activated using either KOH or H_3PO_4. The efficiency of the electrodes examined in the Li half-cell by GCD, CV, and EIS demonstrated that PAC activated by H_3PO_4 exhibits greater capacity at lower c-rates, while PAC activated by KOH exhibits improved reversible capacity at high currents, with efficiency approaching 100 % during initial cycles and reversible capacity exceeding 175 mA h g^{-1}. As a result, the carbons and $LiFePO_4$ cathode are coupled to create Li^+ cells that can generate 160 mA per hour per square volt at 2.8 V with a retention rate that exceeds 95 % after 200 cycles at the C/3 rate. As a result, carbons are recommended as an environmentally friendly anode for Li^+ batteries.

Yu et al. [135] have developed a quick and simple approach for creating an PAC anode from rice husk utilizing NaOH as an activator, which is essential for creating a high hierarchical porosity structure. In comparison to non-activated rice husk carbon (RHC, 5 m^2 g^{-1}), the rice husk activated carbon (RHAC) sample has a larger specific surface area of 2176 m^2 g^{-1}. Because mesopores and macropores co-exist in RHAC with an adsorption average pore width of 2.54 nm, after 100 cycles at a charge of 0.2C with a reversible capacity at 448 mA h g^{-1} for RHAC. Therefore, compared with RHC, RHAC could be attributed to the hierarchical porous structure with more edges, defects, and an enlarged surface area [135]. Boonprachai et al. [118] have also prepared a natural PAC calcined at 500 °C for 1 h derived from popped rice under nitrogen flow as anode materials for Li^+ batteries, as indicated in Fig. 13(a) and (b). The materials were activated by KOH, $ZnCl_2$, $FeCl_3$, and Mg and got PAC. After chemical activation again, the carbon is exposed to heating activation at 800 °C for 3 h under nitrogen gas flow and can be labeled as PAC-KOH, PAC-$ZnCl_2$, PAC-$FeCl_3$, and PAC-Mg (see Fig. 13 (c–f)). After the activation process, interconnected macropores, additional micropores, and mesopores were found in all PAC products. The PAC, which was activated by KOH (PAC-KOH), possessed the largest surface area of 1695.58 m^2 g^{-1} and pore volume of 0.9442 cm^3g^{-1} (see Fig. 13(g) and (h)). This contributed to excellent electrochemical performance, as evidenced by the highest capacity value of 383 mA h g^{-1} for 150 cycles at a current density of 100 mA g^{-1} (Fig. 13(i)). The special attractiveness of such interconnected porous networks has the ability of mass mobilization and accessibility within porous structures with increases in the local uptake rate of Li^+ [118].

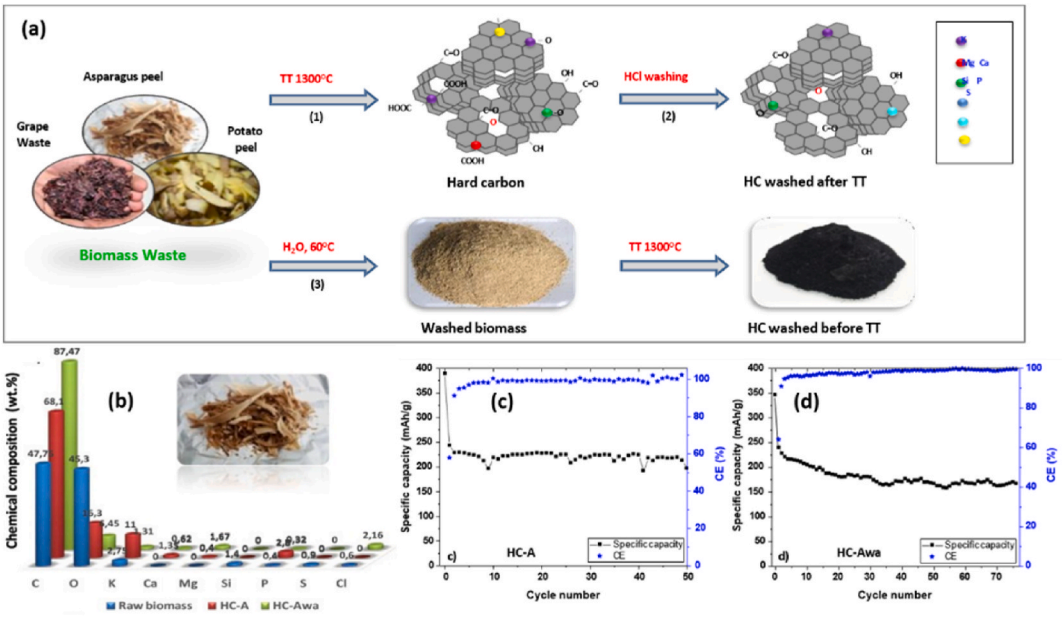

Fig. 14. (a) Synthesis routes used to prepare hard carbons derived from raw biomass precursors: [(1) pristine HC, (2) HC washed after the TT, (3) HC washed before the TT]. (b) Asparagus Chemical composition determined by EDX for biomass precursors, hard carbons and washed hard carbons after pyrolysis, and Long term cycling along with CE of asparagus derived HC. (c) Pristine. (d) Washed. [HC = Hard carbon, TT = Thermal treatment, CE = coulombic efficiency, HC-A = Hard carbon of Asparagus peel before washing, HC-Awa = Hard carbon of Asparagus peel after washing]. Reproduced with permission from Ref. [117]. Copyright 2020 Elsevier.

3.2.2. Sodium-ion

The deficiency issues with Li^+ batteries have recently brought sodium-ion (Na^+) batteries a lot more attention. The main problems with Li^+ based batteries were found to be the existing of safety concerns, the high energy demand caused by the quick development of electric cars, and the potential depletion of Li supplies. To solve this, metal oxides, alloys, sulfides and phosphates, organic compounds, 2D materials and graphite and non-graphite anodic materials have been the most recently investigated to improve the properties of the anode and then enhance the power efficiency [136]. As a result, hard carbon materials have drawn more attention for the development of effective anode materials for efficient Na^+ batteries because of their low-cost, high availability, adjustable characteristics, and theoretical capacity that is close to graphite. Because of this, a variety of synthetic precursors, such as phenolic resin, polyacrylonitrile, and polyaniline, as well as bio-polymers, such as cellulose, sucrose, glucose, and lignin, are employed to create hard carbons [117]. To brief more, Beda et al. [117] have reported the preparation of hard carbon materials derived from different raw biomass precursors and their detailed synthesis routes. Asparagus biomass precursor's hard carbons had the highest chemical composition, as assessed by EDX, following pyrolysis, with values of 87.47 %, compared to grape and potato, which had values less than 87.00 % (Fig. 14(a) and (b)). The results of additional cycles of testing at a C/10 rate on HC-A and HC-Awa. While the CE achieves 100 % after the first 5 cycles, the HC-A capacity was extremely consistent in the first 50 cycles, with the exception of a few minor local changes (Fig. 14(c) and (d)). One can observe how the capacity steadily drops off during the first approximation in the case of the washed sample, HC-Awa. After 35 cycles, it stabilizes at a fairly steady value. Around cycle 30, the CE progressively increases to 100 % and then essentially stays the same during the following cycles.

3.2.3. Lithium-sulfur

Lithium-sulfur (Li-S)-based batteries have a sophisticated use for biomass-derived PAC using host materials. However, the Li-S system has not been widely available on the commercial market due to several problems during its development, such as the presence of poor conductivity of S, volume changes caused by the reversible reaction of S ⇋ Li_2S_x (x = 1, 2), and the solubility of lithium polysulfides (LiPSs) in the electrolyte solvent. The development of the redox shuttle effect occurs when the LiPSs diffuse to the anode, where they are reduced to short-chain polysulfides, and then diffuse back to the cathode electrode, where long-chain polysulfides are once again created. The provided capacity, CE, and cycle life of the battery are all reduced as a result of all these challenges. In detail, during discharge, the reactions in the positive electrode are started by elemental sulfur reduction into longer LiPSs, Li_2S_x (x = 4–8), which dissolve to different degrees in different electrolytes by including commonly used ether-based electrolytes, as shown in Fig. 15 (a) and (b). To enable the electrochemical reactions, the fully charged and discharged states' insulating properties necessitate a conductive matrix in the positive electrode. Creating S/C composite electrodes out of very PAC is a common way to do this [137].

The aforementioned problems have been continued by employing high-energy-density Li-S batteries to offer greater energy storage and quicker power delivery [138]. Particularly, the insulating properties of S and the frequent dissolution of polysulfide intermediates cause rapid capacity degradation in the Li-S system. These behaviors have also been a reflection of the low energy density in supercapacitors. So, in order to increase the potential of the sulfur cathode and capture the dissolved LiPSs, biomass-based PAC with high conductivity and adequate porosity has been employed to host sulfur [138]. For example, Liu et al. [139] have made PAC out of coconut shells by carbonizing them following KOH activation. According to the report, the produced PAC displayed a high specific surface area of 2258.7 $m^2\ g^{-1}$ with an average pore size of 2.246 nm and a mainly covered microporous structure with tiny mesoporous

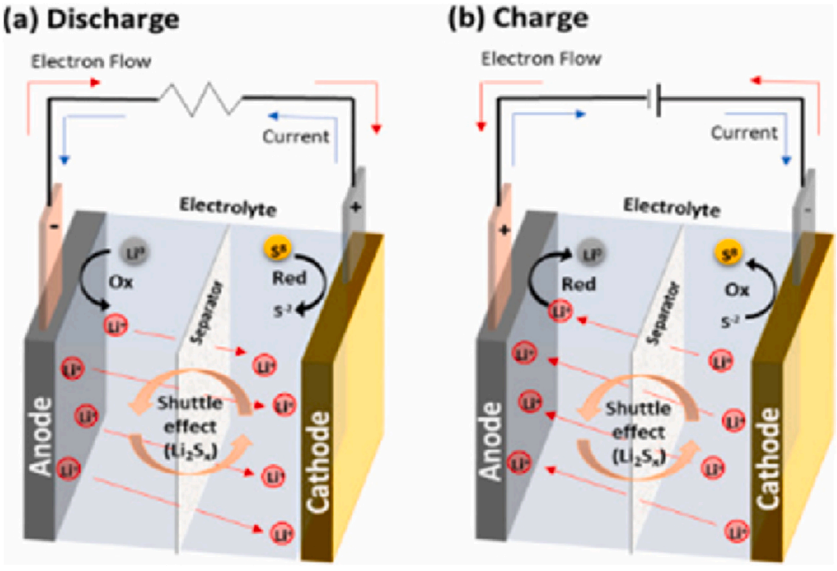

Fig. 15. (a) Components and mode of operation in discharge. (b) Charge for a Li-S battery. Reproduced with permission from Ref. [137]. Copyright 2021 Elsevier.

inclusions. In its Li-S battery applications, 60 % of the S was placed into the PAC and converted to cathode. At first, a current density of 200 mA g^{-1} was used to provide a maximum discharge capacity of 1233 mA h g^{-1}. This occurred because the cell retained 929 mA h g^{-1} with 80 % capacity retention of the initial discharge after 100 cycles, which was caused by the strong absorption force of the micropores and high pore volume. It was also discovered that the pore volume of carbon material held greater significance than its surface area. It seems that the pore volume in the metal-air battery cathode contributes to the accommodation of the discharge product [140].

However, the conductivity is reduced, and the ion transport channel to the active materials is destroyed due to the weak contact between the active sulfur and the conductive additives in Li-S. To solve this, Fan et al. [141] have created a 3D conductive microstructure that helps to be best in self-supporting S storage and good electron-ion transport channels during Li-S batteries as cathode devices. Here, a 3D reticulated and self-supporting carbon framework (SCF) carrier made of carbonized and activated pomelo peels is used to fabricate SCF@rGO, a self-supporting and binder-free cathode with a high capacity of 1675 mA h g^{-1}. Next, SCF@rGO is filled with reduced graphene oxide (rGO) and hierarchically channeled with high S areal loading (see Fig. 16(a)). The samples' layering and wrinkled morphology are evident in their microstructure, which preserves the skeleton and groove structure of pomelo peels in their original state, as shown in Fig. 16(b–g). The microstructure's wrinkly and lamellar characteristics are amazingly helpful in maximizing the particular surface area [141]. Because of its inexpensive cost and high energy conversion efficiency, this AC is a viable electrode for future Li-S batteries.

3.2.4. *Aluminium-air*

An inexpensive and storable material with quick interconvertible capabilities should have been favored at any time or location to increase the utilization of energy conversion and storages. It is continued that the high cost of Pt places a significant obstacle in the way of widespread use of their Pt-based electrode catalysts. Additionally, this produces an increase in the cell's overpotential since Pt is used in reduction-oxidation mechanisms to deal with the slow ORR kinetics on the cathode of aluminum-air (Al-air) batteries during discharge. These characteristics can reduce the battery's round-trip efficiency. As a result, significant efforts have been made to identify affordable, sustainable, and alternative approaches to ORR catalysis. Hence, Sumboja et al. [56] have reported a high-performance, cost-effective ORR catalyst for the commercialization of Al-air batteries with high energy density and low production costs. According to their paper, a catalyst was made by pyrolyzing pistachio or peanut shell waste based carbon, adding FeCo alloy NPs, and nitrogen doping all at once. Combining physical and chemical treatments on the biomass allowed for the production of pistachio shell-derived PAC with a sizable surface area of 1246.4 m^2 g^{-1}. FeCo/N-C-Pistachio has higher content of N, Fe, and Co with larger electroactive surface area than FeCo/N-C-Peanut catalyst. The resultant catalyst (FeCo/N-C-Pistachio) has a higher content of N,

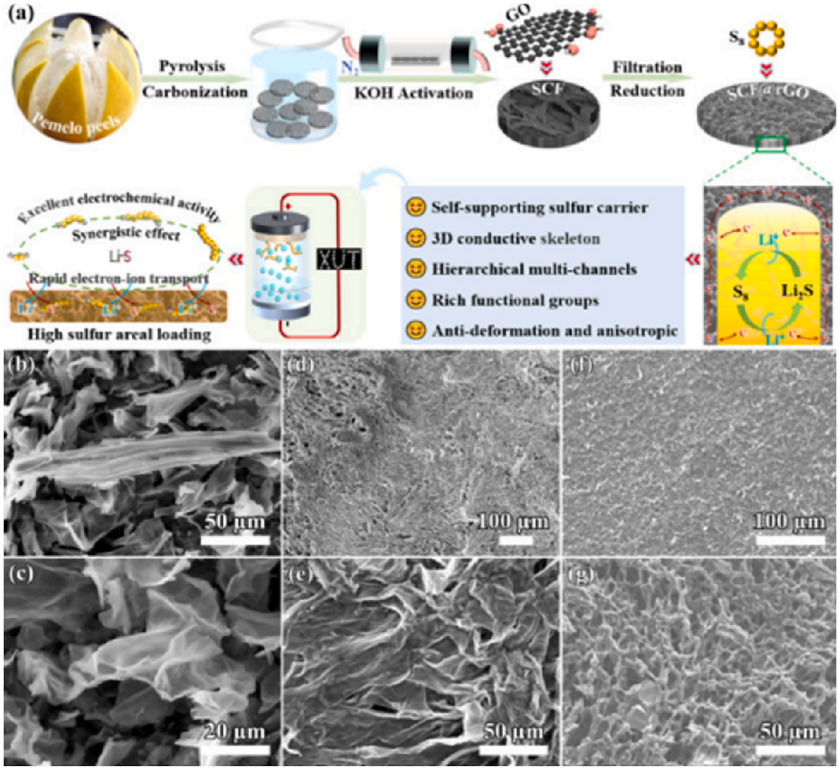

Fig. 16. (a) Schematic diagram for the preparation of SCF@rGO/S cathode and its Li-S battry performance. (b and c) SEM images of PPC. (d and e) SEM images of SCF. (f and g) SEM images of SCF@rGO. Reproduced with permission from Ref. [141]. Copyright 2021 Elsevier.

Fe, and Co, and a larger electrochemically active surface area than its peanut shell counterpart (FeCo/N-C-Peanut). From this, doping with nitrogen increases the number of nucleation sites for FeCo alloy growth that are provided by the large surface area of carbon. Its high ORR activity is indicated by the FeCo/N-C-Pistachio's promising 0.93 V vs. RHE onset potential and 4.49 mA cm^{-2} saturating current density. An Al-air battery with a FeCo/N-C-Pistachio catalyst on the cathode and a commercial Al 1100 anode can operate for 5 h with a consistent discharge voltage of 1.37 V and a power density of 99.7 mW cm^{-2}. This eco-friendly, high-performance electrocatalyst has the potential to play a significant role in the widespread adoption of Al-air batteries.

Because of their well-developed tailored textures (closed pores and defects) and large microcrystalline interlayer spacing, carbon materials derived from biomass have garnered significant attention as effective and sustainable electrode/anode candidates for metal-ion chemistries. This opens up new applications for these materials in environmentally friendly aluminum batteries [21]. The high cost of air cathode catalysts and metal anode device is the main problem in limits the widely application of Al-air batteries. However, to minimize the mentioned drawback, a combination of recycled PAC and rice husk have a solution to modify anode electrode as an alternative modifier for recycled aluminum foil [142]. The material is commonly available material and suitable in Al-air battery due to feasible production cost. Thus, using the modified cathode a voltage of 0.68–0.72 V was produced with 100 % similar activities to PAC battery as a cathode.

3.2.5. *Zinc-air*

Devices that use zinc-air (Zn-air) batteries use electrocatalysts that are both effective and affordable for ORR. Zn-air is regarded as a representative and crucial component for scalable use in metal-air batteries and even in fuel cells. In a metal-air battery, the alteration of the cathode for ORR often improves energy conversion efficiency. Hence, Li et al. [143] have suggested a cathode electrode for zinc-air batteries modified by iron-based nitrogen-doped carbon catalysts (Fe-N-C_{wood}). An approach called hydrothermal driven pyrolysis was used to create the catalyst. The nitrogen-doped carbon obtained from treated wood was employed as a support. This support had a macro-meso-micro hierarchical porous network structure and a sizable specific surface area. This structure ensures that the Zn-air battery's charge-discharge mechanism can mass transfer oxygen species and electrolytes quickly. Fe-N-C_{wood} catalyst showed outstanding activity during its ORR electrochemical test, yielding a half-wave potential of 0.90 V in 0.1 M KOH electrolyte, which was superior to that of 0.70 V in 0.1 M $HClO_4$ electrolyte. Tests on durability also showed that Fe-N-C_{wood} had a good degree of stability and methanol tolerance. The Fe-N-C_{wood} based Zn-air battery therefore produced a maximum peak power density of 231 mW cm^{-2}, indicating its potential use in sustainable energy conversion systems (Fig. 17(a–h)). However, these batteries have a number of drawbacks, including a reliance on ambient conditions, a propensity to dry up when exposed to air, flooding potential, a finite output, and a brief active life. As a result, various improvements have been carried out successfully [144,145].

3.2.6. *Lithium-O_2*

An efficient metal-free cathode electrode function is also built into a hierarchical PAC framework made from biomass that is used in metal-O_2/air batteries [146]. For example, Arjunan et al. [147] have prepared PAC from betel nuts that was carbonized at 800 °C for 3 h with a heating rate of 10 °C min^{-1} in a tubular furnace. This PAC showed a high specific surface area of 768 m^2 g^{-1} and an ordered and merging tube-like porous morphology. KOH was used to chemically activate the carbonized material, and the finished carbon was then combined with 1M HCl to eliminate any remaining unreacted KOH and inorganic impurities. It is possible to store the discharge product of Li_2O_2 in lithium-O_2 (Li-O_2) batteries thanks to the presence of both meso and microporous structure, which result in a well-developed 3D interconnected carbon framework and offer an effective path for the diffusion of the reactant (oxygen as well as air). Because of this, it displays great performance activities and a high specific capacity. It is possible to reach a maximum discharge capacity of 9560 mA h g^{-1} for oxygen and 2000 mA h g^{-1} for ambient air, respectively, at a current density of 100 mA g^{-1}. The produced material also demonstrates 27 cycles of reversible cyclic stability with a specific capacity of 1000 mA h g^{-1} at a current density of 100 mA g^{-1} in an oxygen atmosphere (see Fig. 18).

Zhao et al. [148] have also shown that loose carbon nanosphere clusters generated from biomass are a suitable cathode material for high performance Li-O_2 batteries. The produced carbon compounds have very low concentrations of oxygen and structural flaws on their surfaces, which lessens the side reactions related to carbon degradation. The carbon electrode has an exceptionally with best in specific capacity 20300 mA h g^{-1} and long cycle life at a capacitance retention of 100 % for 543 cycles due to variety of pore structure with modified surface area.

In general, the role of different biomass based PAC and its efficiency in different batteries are summarized in Table 2.

However, the practical application of PAC electrode materials in energy conversion and storage devices are limited due to their low conductivity and rare storage sites in battries and supercapacitor, and low diffusion kinetics. Therefore, various strategies have been designed and developed for the modification of PAC material structures to overcome the mentioned problems. In this review, as a direction from many literature support, numerous issues remain to be resolved in biomass based PAC, these are: i) more research is still needed on the preparation technique by controlling major variables that influences the structure of PAC materials because of the difference in abundance of biomass resources and the wide variations in the content of various biomass raw materials, ii) Materials produced from biomaterials still have inadequate electrochemical performance due to the unformation of excellent structure, low electrical conductivity, and weak stability in low-cost biomass raw materials. As result, furthure required investigation through compound doping of various atoms and surface modification must be needed [138,161,162]. In general, PAC materials have a broad future scope in energy conversion and storage systems, as illustrated in Fig. 19.

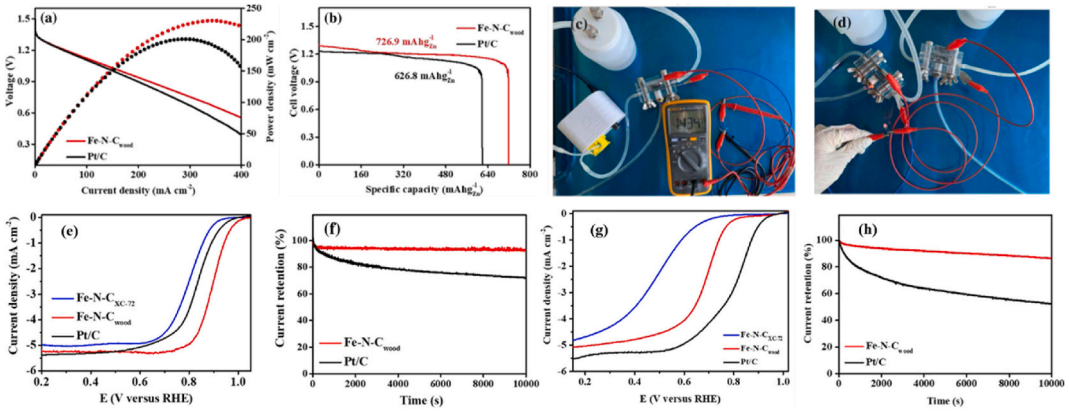

Fig. 17. (a) Discharge polarization and corresponding power density plots of Fe-N-C_{wood} and Pt/C based Zn-air battery. (b) Specific capacities of Fe-N-C_{wood} and Pt/C-based Zn-air battery. (c) Fe-N-C_{wood} based liquid Zn–air battery. (d) LED powered by two liquid Zn-air batteries with the Fe-N-C_{wood} heterostructures electrocatalyst of Zn-air battery performance of Fe-N-C_{wood}. (e) Corresponding Tafel plots. (f) Chronoamperometric response of Fe-N-C_{wood} and Pt/C in O_2-saturated 0.1 M KOH while. (g) Corresponding Tafel plots. (h) Chronoamperometric response of Fe-N-Cwood and Pt/C in O_2-saturated 0.1 M $HClO_4$. Reproduced with permission from Ref. [143]. Copyright 2021 Springer.

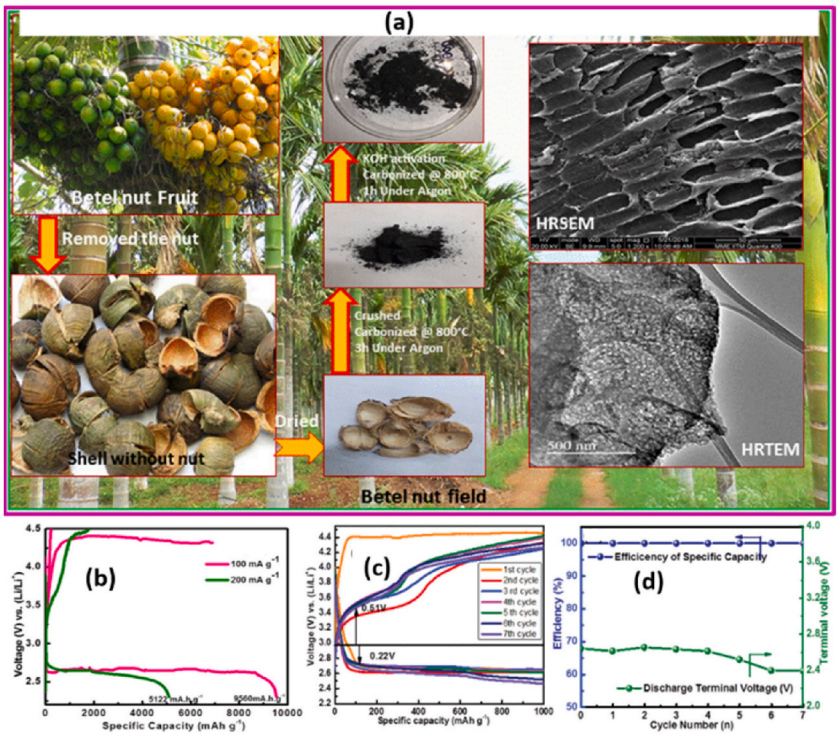

Fig. 18. (a) Preparation procedure. (b) Discharge and charge profile at a current density of 100 and 200 mA/g for Li-O_2 battery in oxygen atmosphere. (c) Cycling stability as cathode material for Li-air battery in an ambient air. (d) The corresponding typical discharge/charge profiles for betel nut derived PAC material. Reproduced with permission from Ref. [147]. Copyright 2021 Wiley.

4. Conclusions and future perspectives

The decline of environmentally damaging non-renewable energy sources like fossil fuels has made way for the emergence of a new era of energy technology. The creation of efficient porous materials like PAC-based composite materials, both as anode and cathode components, demonstrated a high degree of efficiency for the generation and storage of sustainable green energy. Since the surface characteristics and charge transfer kinetics are improved by combining AC with other materials, such as conductive polymers, nanoscale metals, metal oxides, and their composites, the manufacture of electrodes for fuel cells, batteries, and even supercapacitor applications using these types of modified materials is quite selective.

Table 2
Summary of efficiency of biomass derived PAC in different battery device system.

Biomass sources	Battery type	Role	Capacity (mAh g^{-1})	Retention	Reference
Cherry pit	Lithium-ion	Anode	160	95 % at 2.8 V, after 200 cycles	[121]
Rice husk	Lithium-ion	Cathode	17 at 100 mA g^{-1}	at 2.5 V after 500 cycles	[11]
Rice husk	Lithium-ion	Anode	~253	~81 %, after 400 cycles	[149]
Agar	Lithium-ion	Anode	320	at 0.1C after 100 cycles	[150]
Bagasse	Lithium-ion	Anode	325 at 100 mA g^{-1}	after 100 cycles	[151]
Apple	Lithium-ion	Anode	1050 at 100 mA g^{-1}	after 200 cycles	[152]
Celery	Lithium-ion	Anode	990 at 100 mA g^{-1}	after 200 cycles	[152]
Borassus flabellifer	Sodium-ion	Anode	332 at 20 mA g^{-}	86.4 %, after 500 cycles	[153]
Apple	Sodium-ion	Anode	438	after 200 cycles	[152]
Celery	Sodium-ion	Anode	451	after 200 cycles	[152]
Brewer's spent grain	Sodium-ion	Anode	296 at 50 mA g^{-1}	86.4 %, after 400 cycles	[154]
Rice husk	Lithium-Sulfur	Cathode	1230 and 970	at 0.1C and 0.2C after 100 cycles	[11]
Milk waste	Lithium-Sulfur	Separator/cathode	495.2	At 100 cycle	[155]
Coconut shells	Lithium-Sulfur	Cathode	929	80 %, after 100 cycles	[139]
Peanut shell	Lithium-Sulfur	Cathode	619	95 %, at 0.2C, after 100 cycles	[156]
Pomelo peel	Lithium-Sulfur	Cathode	750	96 %, at 2C, after 100 cycles	[157]
Chitin	Aluminium-air	Cathode	32.24 mW cm^{-2} at 20 mA cm^{-2}	At a discharge voltage of 1.17 V	[158]
Wheat straw	Zinc-air	Cathode	740.7	90.3 %	[159]
Poplar inflorescence	Lithium-O_2	Cathode	12060 at 0.02 mA cm^{-2}	At an average voltage of 2.8 V	[160]

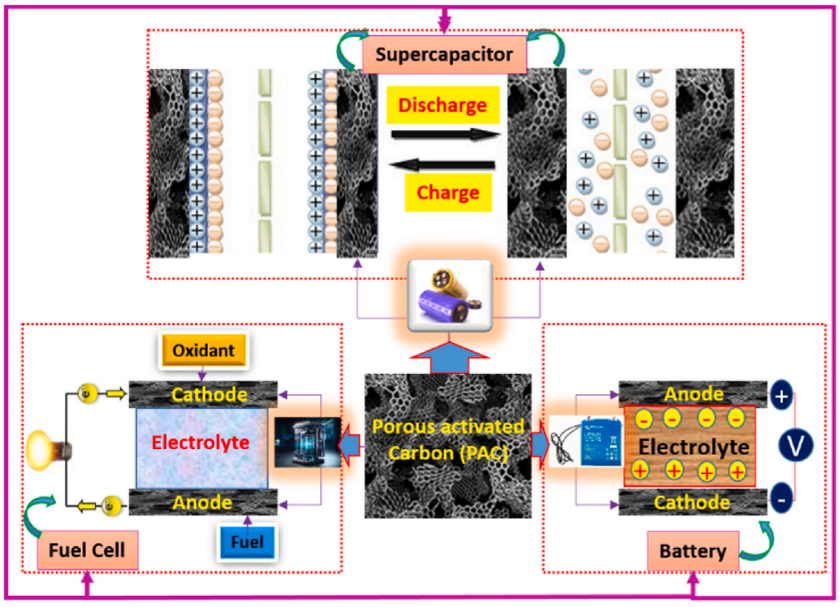

Fig. 19. Future scope illustration of the biomass-based PAC materials in supercapacitor, fuel cell, and battry devicees.

The PAC and their composites were discovered to show improvements in the manufacturing of modified components for energy generation and conversion, as can be summarized and evaluated in this review. However, as evidenced by recent studies, commercialization and domestic use of batteries, fuel cells, and supercapacitors are not yet widespread and pronounced habits. This may be related to the energy obtained from such sources' low efficiency. Batteries, fuel cells, and supercapacitors are studied and their performance enhanced with the use of an effective PAC and its composite-based electrode. Consequently, it is evident from this review that batteries, fuel cells, and supercapacitors are emerging technologies for energy conversion and storage because of the recent remarkable advancements in electrode materials, which have improved their performance to a great extent in energy conversion and storage systems.

Significant progress has been made in the past few years toward creating PAC materials derived from biomass that can be used as electrodes for batteries, fuel cells, and supercapacitors. Nonetheless, there are a number of significant technological and practical obstacles that must be addressed. These include challenges in choosing appropriate and suitable methods for preparing carbon and biomass, problems in managing and customizing pore size and geometry, a deeper comprehension of SSA, pore structure with volume mechanisms, and electrochemical effects. Because of their affordability, environmental friendliness, and intrinsic qualities, PAC generated from biomass are anticipated to be a desirable substitute for creating and constructing novel electrochemical energy conversion and energy storage systems. Hence, the environmentally friendly, economically viable, and renewable PAC preparation will be

a valuable raw material for the production of cutting-edge energy conversion and storage devices. Therefore, for different energy conversion and energy storage systems using PAC derived from biomass as electrodes to become commercially viable, large-scale synthesis processes must be developed. Future development will mostly focus on using renewable resources as raw materials to create energy conversion and storage devices with great efficiency.

CRediT authorship contribution statement

Yilkal Dessie: Writing – review & editing, Writing – original draft, Methodology, Conceptualization. **Eneyew Tilahun:** Writing – review & editing, Visualization, Supervision, Conceptualization. **Tadele Hunde Wondimu:** Writing – original draft, Visualization, Supervision, Conceptualization.

Data availability statement

All the data are available in this work and no additional data was described in the revirew article.

Ethics statement

All statements obtained from all authors were followed rules, guidelines, and regulations.

Declaration of competing interest

The authors declare that they have no known competing financial interests or personal relationships that could have appeared to influence the work reported in this paper.

Acknowledgements

The authors acknowledged Adama Science and Technology University, Ethiopia for financial support.

References

[1] N. Kumar Komal, P. Kumar Singh, R. Singh, V. Kumar Shukla, 'Kusha' (eragrostis cynosuroids): a source of activated carbon for energy storage device, Mater. Today Proc. 34 (2021) 702–704, https://doi.org/10.1016/j.matpr.2020.03.723.
[2] B.K. Kim, S. Sy, A. Yu, J. Zhang, Electrochemical supercapacitors for energy storage and conversion, Handb. Clean Energy Syst (2015) 1–25, https://doi.org/10.1002/9781118991978.hces112.
[3] M. Winter, R.J. Brodd, What are batteries, fuel cells, and supercapacitors? Chem. Rev. 104 (2004) 4245–4269, https://doi.org/10.1021/cr020730k.
[4] D. Nagpal, A. Singh, A. Vasishth, R. Singh, A. Kumar, Electrochemical evaluation of hybrid La2CoCrO6/Co3O4/rGO composite for enhanced supercapacitor performance, Carbon Trends 15 (2024) 100358, https://doi.org/10.1016/j.cartre.2024.100358.
[5] S.K. Bhatia, H.S. Joo, Y.H. Yang, Biowaste-to-bioenergy using biological methods – a mini-review, Energy Convers. Manag. 177 (2018) 640–660, https://doi.org/10.1016/j.enconman.2018.09.090.
[6] E.W. Gabisa, S.H. Gheewala, Potential of bio-energy production in Ethiopia based on available biomass residues, Biomass Bioenergy 111 (2018) 77–87, https://doi.org/10.1016/j.biombioe.2018.02.009.
[7] I.G.B.N. Makertihartha, M. Zunita, Z. Rizki, P.T. Dharmawijaya, Recent advances on Zeolite modification for direct alcohol fuel cells (DAFCs), in: AIP Conf. Proc. (2017) 020030, https://doi.org/10.1063/1.4976894.
[8] Y. Cheng, L. Wu, C. Fang, T. Li, J. Chen, M. Yang, Q. Zhang, Synthesis of porous carbon materials derived from laminaria japonica via simple carbonization and activation for supercapacitors, J. Mater. Res. Technol. 9 (2020) 3261–3271, https://doi.org/10.1016/j.jmrt.2020.01.022.
[9] P. Wei, M. Abid, H. Adun, D. Kemena Awoh, D. Cai, J.H. Zaini, O. Bamisile, Progress in energy storage technologies and methods for renewable energy systems application, Appl. Sci. 13 (2023) 5626, https://doi.org/10.3390/app13095626.
[10] L. Rajeshkumar, M. Ramesh, V. Bhuvaneswari, D. Balaji, Carbon nano-materials (CNMs) derived from biomass for energy storage applications: a review, Carbon Lett 33 (2023) 661–690, https://doi.org/10.1007/s42823-023-00478-3.
[11] K. Chen, D. Xue, Multiple functional biomass-derived activated carbon materials for aqueous supercapacitors, lithium-ion capacitors and lithium-sulfur batteries, Chinese J. Chem. 35 (2017) 861–866, https://doi.org/10.1002/cjoc.201600785.
[12] M. Vinayagam, R. Suresh Babu, A. Sivasamy, A.L.F. de Barros, Biomass-derived porous activated carbon nanofibers from Sapindus trifoliatus nut shells for high-performance symmetric supercapacitor applications, Carbon Lett 31 (2021) 1133–1143, https://doi.org/10.1007/s42823-021-00235-4.
[13] E. Taer, N. Yanti, W.S. Mustika, A. Apriwandi, R. Taslim, A. Agustino, Porous activated carbon monolith with nanosheet/nanofiber structure derived from the green stem of cassava for supercapacitor application, Int. J. Energy Res. 44 (2020) 10192–10205, https://doi.org/10.1002/er.5639.
[14] Z. Zhai, L. Zhang, T. Du, B. Ren, Y. Xu, S. Wang, J. Miao, Z. Liu, A review of carbon materials for supercapacitors, Mater. Des. 221 (2022) 111017, https://doi.org/10.1016/j.matdes.2022.111017.
[15] A. Jana, R. Paul, A.K. Roy, Architectural Design and Promises of Carbon Materials for Energy Conversion and Storage: in Laboratory and Industry, Elsevier Inc., 2019, https://doi.org/10.1016/B978-0-12-814083-3.00002-0.
[16] S. Rajagopal, R. Pulapparambil Vallikkattil, M. Mohamed Ibrahim, D.G. Velev, Electrode materials for supercapacitors in hybrid electric vehicles: challenges and current progress, Condens. Matter. 7 (2022) 6, https://doi.org/10.3390/condmat7010006.
[17] G. Xu, C. Zhu, G. Gao, Recent progress of advanced conductive metal–organic frameworks: precise synthesis, electrochemical energy storage applications, and future challenges, Small 18 (2022) 2203140, https://doi.org/10.1002/smll.202203140.
[18] D. Salinas-Torres, R. Ruiz-Rosas, E. Morallón, D. Cazorla-Amorós, Strategies to enhance the performance of electrochemical capacitors based on carbon materials, Front. Mater. 6 (2019) 1–24, https://doi.org/10.3389/fmats.2019.00115.
[19] Komal, R. Singh, V.G. Parale, Y. Kumar, K. Mishra, V.K. Shukla, Studies on the ZnCl2 activated carbons derived from Sabal palmetto and Pterospermum acerifolium leaves for EDLC application, Biomass Convers. Biorefinery 14 (2024) 9995–10009, https://doi.org/10.1007/s13399-022-03088-7.
[20] F. Yu, S. Li, W. Chen, T. Wu, C. Peng, Biomass-derived materials for electrochemical energy storage and conversion: overview and perspectives, Energy Environ. Mater. 2 (2019) 55–67, https://doi.org/10.1002/eem2.12030.

[21] G.S. Dos Reis, S. Petnikota, C.M. Subramaniyam, H.P. de Oliveira, S. Larsson, M. Thyrel, U. Lassi, F. García Alvarado, Sustainable biomass-derived carbon electrodes for potassium and aluminum batteries: conceptualizing the key parameters for improved performance, Nanomaterials 13 (2023) 765, https://doi.org/10.3390/nano13040765.
[22] G.S. Dos Reis, S.H. Larsson, H.P. de Oliveira, M. Thyrel, E.C. Lima, Sustainable biomass activated carbons as electrodes for battery and supercapacitors–a mini-review, Nanomaterials 10 (2020) 1–22, https://doi.org/10.3390/nano10071398.
[23] S. Ghosh, R. Santhosh, S. Jeniffer, V. Raghavan, G. Jacob, K. Nanaji, P. Kollu, S.K. Jeong, A.N. Grace, Natural biomass derived hard carbon and activated carbons as electrochemical supercapacitor electrodes, Sci. Rep. 9 (2019) 16315, https://doi.org/10.1038/s41598-019-52006-x.
[24] D. Nagpal, A. Singh, A. Vasishth, R. Singh, A. Kumar, Effect of redox additive in aqueous electrolyte for electrochemical energy storage applications of A and B site ordered LaCaCoCrO 6 double perovskite, Phys. Status Solidi. 220 (2023) 1–10, https://doi.org/10.1002/pssa.202300495.
[25] R. Li, Y. Zhou, W. Li, J. Zhu, W. Huang, Structure engineering in biomass-derived carbon materials for electrochemical, Energy Storage, Research 2020 (2020) 1–27, https://doi.org/10.34133/2020/8685436.
[26] B.X. Zou, Y. Wang, X. Huang, Y. Lu, Hierarchical N- and O-Doped porous carbon composites for high-performance supercapacitors, J. Nanomater. 2018 (2018), https://doi.org/10.1155/2018/8945042.
[27] J.L. Goldfarb, G. Dou, M. Salari, M.W. Grinstaff, Biomass-based fuels and activated carbon electrode materials: an integrated approach to green energy systems, ACS Sustain. Chem. Eng. 5 (2017) 3046–3054, https://doi.org/10.1021/acssuschemeng.6b02735.
[28] K. Januszewicz, P. Kazimierski, M. Klein, D. Kardaś, J. Łuczak, Activated carbon produced by pyrolysis of waste wood and straw for potential wastewater adsorption, Materials 13 (2020) 1–13, https://doi.org/10.3390/MA13092047.
[29] Z. Zhang, H. Zhao, W. Gu, L. Yang, B. Zhang, A biomass derived porous carbon for broadband and lightweight microwave absorption, Sci. Rep. 9 (2019) 1–10, https://doi.org/10.1038/s41598-019-54104-2.
[30] K. Wu, B. Gao, J. Su, X. Peng, X. Zhang, J. Fu, S. Peng, P.K. Chu, Large and porous carbon sheets derived from water hyacinth for high-performance supercapacitors, RSC Adv. 6 (2016) 29996–30003, https://doi.org/10.1039/C5RA25098F.
[31] A. Wang, Z. Zheng, R. Li, D. Hu, Y. Lu, H. Luo, K. Yan, Biomass-derived porous carbon highly efficient for removal of Pb(II) and Cd(II), Green Energy Environ. 4 (2019) 414–423, https://doi.org/10.1016/j.gee.2019.05.002.
[32] C. Song, B. Zhang, L. Hao, J. Min, N. Liu, R. Niu, J. Gong, T. Tang, Converting poly(ethylene terephthalate) waste into N-doped porous carbon as CO2 adsorbent and solar steam generator, Green Energy Environ. 7 (2022) 411–422, https://doi.org/10.1016/j.gee.2020.10.002.
[33] J. Gong, J. Liu, X. Chen, Z. Jiang, X. Wen, E. Mijowska, T. Tang, Converting real-world mixed waste plastics into porous carbon nanosheets with excellent performance in the adsorption of an organic dye from wastewater, J. Mater. Chem. A. 3 (2015) 341–351, https://doi.org/10.1039/c4ta05118a.
[34] X. Yuan, M.K. Cho, J.G. Lee, S.W. Choi, K.B. Lee, Upcycling of waste polyethylene terephthalate plastic bottles into porous carbon for CF4 adsorption, Environ. Pollut. 265 (2020) 114868, https://doi.org/10.1016/j.envpol.2020.114868.
[35] J. Ma, J. Liu, J. Song, T. Tang, Pressurized carbonization of mixed plastics into porous carbon sheets on magnesium oxide, RSC Adv. 8 (2018) 2469–2476, https://doi.org/10.1039/c7ra12733b.
[36] K. Yan, R. Li, Z. Yang, X. Li, Y. Wang, G. Wu, Biomass waste-derived porous carbon efficient for simultaneous removal of chlortetracycline and hexavalent chromium, iScience 24 (2021) 102421, https://doi.org/10.1016/j.isci.2021.102421.
[37] S.A. Bapat, D.K. Jaspal, Surface-modified water hyacinth (Eichhornia crassipes) over activated carbon for wastewater treatment: a comparative account, South African, J. Chem. 73 (2020) 70–80, https://doi.org/10.17159/0379-4350/2020/V73A11.
[38] M. Sivachidambaram, J.J. Vijaya, L.J. Kennedy, R. Jothiramalingam, H.A. Al-Lohedan, M.A. Munusamy, E. Elanthamilan, J.P. Merlin, Preparation and characterization of activated carbon derived from the: Borassus flabellifer flower as an electrode material for supercapacitor applications, New J. Chem. 41 (2017) 3939–3949, https://doi.org/10.1039/c6nj03867k.
[39] J. Hou, J. Hou, Y. Liu, S. Wen, W. Li, R. Liao, L. Wang, Sorghum-waste-derived high-surface area KOH-activated porous carbon for highly efficient methylene blue and Pb(II) removal, ACS Omega 5 (2020) 13548–13556, https://doi.org/10.1021/acsomega.9b04452.
[40] D. Kobina Sam, E. Kobina Sam, X. Lv, Application of biomass-derived nitrogen-doped carbon aerogels in electrocatalysis and supercapacitors, Chemelectrochem 7 (2020) 3695–3712, https://doi.org/10.1002/celc.202000829.
[41] X.Y. Luo, Y. Chen, Y. Mo, A review of charge storage in porous carbon-based supercapacitors, Xinxing Tan Cailiao/New Carbon Mater. 36 (2021) 49–68, https://doi.org/10.1016/S1872-5805(21)60004-5.
[42] X. Ma, R. Chen, K. Zhou, Q. Wu, H. Li, Z. Zeng, L. Li, Activated porous carbon with an ultrahigh surface area derived from waste biomass for acetone adsorption, CO2Capture, and light hydrocarbon separation, ACS Sustain. Chem. Eng. 8 (2020) 11721–11728, https://doi.org/10.1021/acssuschemeng.0c03725.
[43] A. Sivakami, A. Ganesan, P. Sakthivel, K. Sridharan, S. Venkatachalam, S. Pitchaimuthu, Porous carbon derived from biomass for fuel cells, in: Biomass-Derived Carbon Mater, Wiley, 2022, pp. 229–252, https://doi.org/10.1002/9783527832903.ch10.
[44] A. Gopalakrishnan, S. Badhulika, Effect of self-doped heteroatoms on the performance of biomass-derived carbon for supercapacitor applications, J. Power Sources 480 (2020) 228830, https://doi.org/10.1016/j.jpowsour.2020.228830.
[45] Y. He, X. Zhuang, C. Lei, L. Lei, Y. Hou, Y. Mai, X. Feng, Porous carbon nanosheets: synthetic strategies and electrochemical energy related applications, Nano Today 24 (2019) 103–119, https://doi.org/10.1016/j.nantod.2018.12.004.
[46] D. Chen, H. Zhou, H. Li, J. Chen, S. Li, F. Zheng, Self-template synthesis of biomass-derived 3D hierarchical N-doped porous carbon for simultaneous determination of dihydroxybenzene isomers, Sci. Rep. 7 (2017) 1–10, https://doi.org/10.1038/s41598-017-15129-7.
[47] J. Kim, Y.J. Heo, J.Y. Hong, S.K. Kim, Preparation of porous carbon nanofibers with tailored porosity for electrochemical capacitor electrodes, Materials 13 (2020), https://doi.org/10.3390/ma13030729.
[48] L. Miao, Z. Song, D. Zhu, L. Li, L. Gan, M. Liu, Recent advances in carbon-based supercapacitors, Mater. Adv. 1 (2020) 945–966, https://doi.org/10.1039/d0ma00384k.
[49] Y.X. Gan, Activated Carbon from Biomass Sustainable Sources, C 7 (2021) 39, https://doi.org/10.3390/c7020039.
[50] H. Zhang, X.L. Zhou, L.M. Shao, F. Lü, P.J. He, Hierarchical porous carbon spheres from low-density polyethylene for high-performance supercapacitors, ACS Sustain. Chem. Eng. 7 (2019) 3801–3810, https://doi.org/10.1021/acssuschemeng.8b04539.
[51] J. Ying, R. Yin, Z. Zhao, X. Zhang, W. Feng, J. Peng, C. Liang, Hierarchical porous carbon materials for lithium storage: preparation, modification, and applications, Nanotechnology 35 (2024) 332003, https://doi.org/10.1088/1361-6528/ad4b21.
[52] J. Palomo, M.Á. Rodríguez-Cano, J. Rodríguez-Mirasol, T. Cordero, Biomass-derived activated carbon catalysts for the direct dimethyl ether synthesis from syngas, Fuel 365 (2024) 131264, https://doi.org/10.1016/j.fuel.2024.131264.
[53] M. Amer, A. Elwardany, Biomass carbonization, in: Renew. Energy - Resour. Challenges, Appl., IntechOpen, 2020, p. 13, https://doi.org/10.5772/intechopen.90480.
[54] W. Ananpreechakorn, T. Seetawan, Synthesis and characterization of activated carbon from water hyacinth, J. Phys. Conf. Ser. 2013 (2021) 012025, https://doi.org/10.1088/1742-6596/2013/1/012025.
[55] E.V. Liakos, K. Rekos, D.A. Giannakoudakis, A.C. Mitropoulos, J. Fu, G.Z. Kyzas, Activated porous carbon derived from tea and plane tree leaves biomass for the removal of pharmaceutical compounds from wastewaters, Antibiotics 10 (2021) 1–16, https://doi.org/10.3390/antibiotics10010065.
[56] A. Sumboja, B. Prakoso, Y. Ma, F.R. Irwan, J.J. Hutani, A. Mulyadewi, M.A.A. Mahbub, Y. Zong, Z. Liu, FeCo nanoparticle-loaded nutshell-derived porous carbon as sustainable catalyst in Al-air batteries, Energy Mater. Adv. 2021 (2021) 8–10, https://doi.org/10.34133/2021/7386210.
[57] J. Niu, J. Guan, M. Dou, Z. Zhang, J. Kong, F. Wang, Sustainable synthesis of biomass-derived carbon electrodes with hybrid energy-storage behaviors for use in high-performance Na-ion capacitors, ACS Appl. Energy Mater. 3 (2020) 2478–2489, https://doi.org/10.1021/acsaem.9b02166.
[58] M. Muthu Balasubramanian, M. Subramani, D. Murugan, S. Ponnusamy, Groundnut shell–derived porous carbon-based supercapacitor with high areal mass loading using carbon cloth as current collector, Ionics 26 (2020) 6297–6308, https://doi.org/10.1007/s11581-020-03754-8.

[59] M. Ni, L. Zhou, Y. Liu, R. Ni, Advances in the synthesis and applications of porous carbon materials, Front. Chem. 11 (2023) 1–5, https://doi.org/10.3389/fchem.2023.1205280.

[60] K. Zhang, J. Sun, L. E, C. Ma, S. Luo, Z. Wu, W. Li, S. Liu, Effects of the pore structure of commercial activated carbon on the electrochemical performance of supercapacitors, J. Energy Storage 45 (2022) 103457, https://doi.org/10.1016/j.est.2021.103457.

[61] M. Nasir, Y. Nakanishi, A. Patmonoaji, T. Suekane, Effects of porous electrode pore size and operating flow rate on the energy production of capacitive energy extraction, Renew. Energy 155 (2020) 278–285, https://doi.org/10.1016/j.renene.2020.03.163.

[62] J. Sánchez-Monreal, M. Vera, P.A. García-Salaberri, Fundamentals of electrochemistry with application to direct alcohol fuel cell modeling, Prot. Exch. Membr. Fuel Cell. (2018), https://doi.org/10.5772/intechopen.71635.

[63] M.H. de Sá, A.M.F.R. Pinto, V.B. Oliveira, Passive small direct alcohol fuel cells for low-power portable applications: assessment based on innovative increments since 2018, Energies 15 (2022), https://doi.org/10.3390/en15103787.

[64] S.M. Khantimerov, E.F. Kukovitsky, N.A. Sainov, N.M. Suleimanov, Fuel cell electrodes based on carbon nanotube/metallic nanoparticles hybrids formed on porous stainless steel pellets, Int. J. Chem. Eng. 2013 (2013), https://doi.org/10.1155/2013/157098.

[65] P. Saisirirat, B. Joommanee, Study on the performance of the micro direct ethanol fuel cell (Micro-DEFC) for applying with the portable electronic devices, Energy Proc. 138 (2017) 187–192, https://doi.org/10.1016/j.egypro.2017.10.148.

[66] Y. Dessie, S. Tadesse, R. Eswaramoorthy, B. Abebe, Recent developments in manganese oxide based nanomaterials with oxygen reduction reaction functionalities for energy conversion and storage applications: a review, J. Sci. Adv. Mater. Devices. 4 (2019) 353–369, https://doi.org/10.1016/j.jsamd.2019.07.001.

[67] H. Su, Y.H. Hu, Recent advances in graphene-based materials for fuel cell applications, Energy Sci. Eng. 9 (2021) 958–983, https://doi.org/10.1002/ese3.833.

[68] A.D. Moore, S.M. Holmes, E.P.L. Roberts, Evaluation of porous carbon substrates as catalyst supports for the cathode of direct methanol fuel cells, RSC Adv. 2 (2012) 1669–1674, https://doi.org/10.1039/c1ra01121a.

[69] F. Mohajer, G.M. Ziarani, A. Badiei, S. Iravani, R.S. Varma, MXene-carbon nanotube composites: properties and applications, Nanomaterials 13 (2023) 345, https://doi.org/10.3390/nano13020345.

[70] Y. Wang, Y. Wang, Recent progress in MXene layers materials for supercapacitors: high-performance electrodes, SmartMat 4 (2023), https://doi.org/10.1002/smm2.1130.

[71] R. Gautam, N. Marriwala, R. Devi, A review: study of Mxene and graphene together, Meas. Sensors. 25 (2023) 100592, https://doi.org/10.1016/j.measen.2022.100592.

[72] S. ul Haque, A. Nasar, Inamuddin, M.M. Rahman, Applications of chitosan (CHI)-reduced graphene oxide (rGO)-polyaniline (PAni) conducting composite electrode for energy generation in glucose biofuel cell, Sci. Rep. 10 (2020) 10428, https://doi.org/10.1038/s41598-020-67253-6.

[73] J. Ali, L. Wang, H. Waseem, H.M.A. Sharif, R. Djellabi, C. Zhang, G. Pan, Bioelectrochemical recovery of silver from wastewater with sustainable power generation and its reuse for biofouling mitigation, J. Clean. Prod. 235 (2019) 1425–1437, https://doi.org/10.1016/j.jclepro.2019.07.065.

[74] A.A. Yaqoob, M.N.M. Ibrahim, K. Umar, Biomass-derived composite anode electrode: synthesis, characterizations, and application in microbial fuel cells (MFCs), J. Environ. Chem. Eng. 9 (2021) 106111, https://doi.org/10.1016/j.jece.2021.106111.

[75] D. Liu, R. Wang, W. Chang, L. Zhang, B. Peng, H. Li, S. Liu, M. Yan, C. Guo, Ti3C2 MXene as an excellent anode material for high-performance microbial fuel cells, J. Mater. Chem. A. 6 (2018) 20887–20895, https://doi.org/10.1039/c8ta07305h.

[76] G. Kothandam, G. Singh, X. Guan, J.M. Lee, K. Ramadass, S. Joseph, M. Benzigar, A. Karakoti, J. Yi, P. Kumar, A. Vinu, Recent advances in carbon-based electrodes for energy storage and conversion, Adv. Sci. 10 (2023) 1–50, https://doi.org/10.1002/advs.202301045.

[77] E. Herrero-Hernandez, T.J. Smith, R. Akid, Electricity generation from wastewaters with starch as carbon source using a mediatorless microbial fuel cell, Biosens. Bioelectron. 39 (2013) 194–198, https://doi.org/10.1016/j.bios.2012.07.037.

[78] M.K. Sarma, M.G.A. Quadir, R. Bhaduri, S. Kaushik, P. Goswami, Composite polymer coated magnetic nanoparticles based anode enhances dye degradation and power production in microbial fuel cells, Biosens. Bioelectron. 119 (2018) 94–102, https://doi.org/10.1016/j.bios.2018.07.065.

[79] F. Offei, A. Thygesen, M. Mensah, K. Tabbicca, D. Fernando, I. Petrushina, G. Daniel, A viable electrode material for use in microbial fuel cells for tropical regions, Energies 9 (2016) 1–14, https://doi.org/10.3390/en9010035.

[80] F. Nourbakhsh, M. Mohsennia, M. Pazouki, Nickel oxide/carbon nanotube/polyaniline nanocomposite as bifunctional anode catalyst for high-performance Shewanella-based dual-chamber microbial fuel cell, Bioprocess Biosyst. Eng. 40 (2017) 1669–1677, https://doi.org/10.1007/s00449-017-1822-y.

[81] B. Bian, D. Shi, X. Cai, M. Hu, Q. Guo, C. Zhang, Q. Wang, A.X. Sun, J. Yang, 3D printed porous carbon anode for enhanced power generation in microbial fuel cell, Nano Energy 44 (2018) 174–180, https://doi.org/10.1016/j.nanoen.2017.11.070.

[82] W. Yang, S. Chen, Biomass-derived carbon for electrode fabrication in microbial fuel cells: a review, Ind. Eng. Chem. Res. 59 (2020) 6391–6404, https://doi.org/10.1021/acs.iecr.0c00041.

[83] Y.H. Hung, T.Y. Liu, H.Y. Chen, Renewable coffee waste-derived porous carbons as anode materials for high-performance sustainable microbial fuel cells, ACS Sustain. Chem. Eng. 7 (2019) 16991–16999, https://doi.org/10.1021/acssuschemeng.9b02405.

[84] S. Kalathil, V.H. Nguyen, J.J. Shim, M.M. Khan, J. Lee, M.H. Cho, Enhanced performance of a microbial fuel cell using CNT/MnO2 nanocomposite as a bioanode material, J. Nanosci. Nanotechnol. 13 (2013) 7712–7716, https://doi.org/10.1166/jnn.2013.7832.

[85] M. Li, S. Ci, Y. Ding, Z. Wen, Almond shell derived porous carbon for a high-performance anode of microbial fuel cells, Sustain. Energy Fuels 3 (2019) 3415–3421, https://doi.org/10.1039/c9se00659a.

[86] G.G. Kumar, C.J. Kirubaharan, S. Udhayakumar, C. Karthikeyan, K.S. Nahm, Conductive polymer/graphene supported platinum nanoparticles as anode catalysts for the extended power generation of microbial fuel cells, Ind. Eng. Chem. Res. 53 (2014) 16883–16893, https://doi.org/10.1021/ie502399y.

[87] X. Xing, Z. Liu, W. Chen, X. Lou, Y. Li, Q. Liao, Self-nitrogen-doped carbon nanosheets modification of anodes for improving microbial fuel cells' performance, Catalysts 10 (2020), https://doi.org/10.3390/catal10040381.

[88] M. Ghasemi, W.R.W. Daud, M. Rahimnejad, M. Rezayi, A. Fatemi, Y. Jafari, M.R. Somalu, A. Manzour, Copper-phthalocyanine and nickel nanoparticles as novel cathode catalysts in microbial fuel cells, Int. J. Hydrogen Energy 38 (2013) 9533–9540, https://doi.org/10.1016/j.ijhydene.2013.01.177.

[89] B. Liang, Y. Zhao, K. Li, C. Lv, Porous carbon codoped with inherent nitrogen and externally embedded cobalt nanoparticles as a high-performance cathode catalyst for microbial fuel cells, Appl. Surf. Sci. 505 (2020) 144547, https://doi.org/10.1016/j.apsusc.2019.144547.

[90] I. Gajda, J. Greenman, I. Ieropoulos, Microbial Fuel Cell stack performance enhancement through carbon veil anode modification with activated carbon powder, Appl. Energy 262 (2020) 114475, https://doi.org/10.1016/j.apenergy.2019.114475.

[91] J. Liu, L. Wei, H. Wang, G. Lan, H. Yang, J. Shen, Biomass-derived N-doped porous activated carbon as a high-performance and cost-effective pH-universal oxygen reduction catalyst in fuel cell, Int. J. Hydrogen Energy 45 (2020) 29308–29321, https://doi.org/10.1016/j.ijhydene.2020.07.216.

[92] S. Karthick, S. Vishnuprasad, K. Haribabu, N.J. Manju, Activated carbon derived from ground nutshell as a metal-free oxygen reduction catalyst for air cathode in single chamber microbial fuel cell, Biomass Convers. Biorefinery 12 (2022) 1729–1736, https://doi.org/10.1007/s13399-021-01335-x.

[93] M. Rethinasabapathy, J.H. Lee, K.C. Roh, S.M. Kang, S.Y. Oh, B. Park, G.W. Lee, Y.L. Cha, Y.S. Huh, Silver grass-derived activated carbon with coexisting micro-, meso- and macropores as excellent bioanodes for microbial colonization and power generation in sustainable microbial fuel cells, Bioresour. Technol. 300 (2020) 122646, https://doi.org/10.1016/j.biortech.2019.122646.

[94] W. Ye, J. Tang, Y. Wang, X. Cai, H. Liu, J. Lin, B. Van der Bruggen, S. Zhou, Hierarchically structured carbon materials derived from lotus leaves as efficient electrocatalyst for microbial energy harvesting, Sci. Total Environ. 666 (2019) 865–874, https://doi.org/10.1016/j.scitotenv.2019.02.300.

[95] M. Li, Y.W. Li, Q.Y. Cai, S.Q. Zhou, C.H. Mo, Spraying carbon powder derived from mango wood biomass as high-performance anode in bio-electrochemical system, Bioresour. Technol. 300 (2020) 122623, https://doi.org/10.1016/j.biortech.2019.122623.

[96] N.A.M. Barakat, S. Gamal, H.Y. Kim, N.M. Abd El-Salam, H. Fouad, O.A. Fadali, H.M. Moustafa, O.H. Abdelraheem, Synergistic advancements in sewage-driven microbial fuel cells: novel carbon nanotube cathodes and biomass-derived anodes for efficient renewable energy generation and wastewater treatment, Front. Chem. 11 (2023) 1–19, https://doi.org/10.3389/fchem.2023.1286572.

[97] N.A.M. Barakat, S. Gamal, H.Y. Kim, N.M. Abd El-Salam, H. Fouad, O.A. Fadali, H.M. Moustafa, O.H. Abdelraheem, Synergistic advancements in sewage-driven microbial fuel cells: novel carbon nanotube cathodes and biomass-derived anodes for efficient renewable energy generation and wastewater treatment, Front. Chem. 11 (2023) 1–19, https://doi.org/10.3389/fchem.2023.1286572.
[98] D. Bose, S. Sridharan, H. Dhawan, P. Vijay, M. Gopinath, Biomass derived activated carbon cathode performance for sustainable power generation from Microbial Fuel Cells, Fuel 236 (2019) 325–337, https://doi.org/10.1016/j.fuel.2018.09.002.
[99] K. Senthilkumar, M. Naveenkumar, Enhanced performance study of microbial fuel cell using waste biomass-derived carbon electrode, Biomass Convers. Biorefinery 13 (2023) 5921–5929, https://doi.org/10.1007/s13399-021-01505-x.
[100] A.A. Yaqoob, M.N.M. Ibrahim, K. Umar, Biomass-derived composite anode electrode: synthesis, characterizations, and application in microbial fuel cells (MFCs), J. Environ. Chem. Eng. 9 (2021) 106111, https://doi.org/10.1016/j.jece.2021.106111.
[101] E. Antolini, E.R. Gonzalez, Alkaline direct alcohol fuel cells, J. Power Sources 195 (2010) 3431–3450, https://doi.org/10.1016/j.jpowsour.2009.11.145.
[102] L. Morales S, J.M. Baas-López, R. Barbosa, D. Pacheco, B. Escobar, Activated carbon from Water Hyacinth as electrocatalyst for oxygen reduction reaction in an alkaline fuel cell, Int. J. Hydrogen Energy 46 (2021) 25995–26004, https://doi.org/10.1016/j.ijhydene.2021.04.094.
[103] P. Piela, R. Fields, P. Zelenay, Electrochemical impedance spectroscopy for direct methanol fuel cell diagnostics, J. Electrochem. Soc. 153 (2006) A1902, https://doi.org/10.1149/1.2266623.
[104] J.H. Bang, K. Han, S.E. Skrabalak, H. Kim, K.S. Suslick, Porous carbon supports prepared by ultrasonic spray pyrolysis for direct methanol fuel cell electrodes, J. Phys. Chem. C 111 (2007) 10959–10964, https://doi.org/10.1021/jp071624v.
[105] G.S. Chai, S.B. Yoon, J.S. Yu, J.H. Choi, Y.E. Sung, Ordered porous carbons with tunable pore sizes as catalyst supports in direct methanol fuel cell, J. Phys. Chem. B 108 (2004) 7074–7079, https://doi.org/10.1021/jp0370472.
[106] D. Hawa Yulianti, D. Rohendi, N. Syarif, A. Rachmat, Performance test of membrane electrode assembly in DAFC using mixed methanol and ethanol fuel with various volume comparison, Indones. J. Fundam. Appl. Chem. 4 (2019) 139–142, https://doi.org/10.24845/ijfac.v4.i3.139.
[107] D.H. Perugupalli, T. Xu, K.T. Cho, Activation of carbon porous paper for alkaline alcoholic fuel cells, Energies 12 (2019) 3207, https://doi.org/10.3390/en12173207.
[108] A. Sarapuu, E. Kibena-Põldsepp, M. Borghei, K. Tammeveski, Electrocatalysis of oxygen reduction on heteroatom-doped nanocarbons and transition metal-nitrogen-carbon catalysts for alkaline membrane fuel cells, J. Mater. Chem. A. 6 (2018) 776–804, https://doi.org/10.1039/c7ta08690c.
[109] T.H.T. Vu, M.D. Nguyen, A.T.N. Mai, Influence of solvents on the electroactivity of PtAl/rGO catalyst inks and anode in direct ethanol fuel cell, J. Chem. 2021 (2021) 1–15, https://doi.org/10.1155/2021/6649089.
[110] Q.X. Li, M.S. Liu, Q.J. Xu, H.M. Mao, Preparation and electrocatalytic characteristics research of Pd/c catalyst for direct ethanol fuel cell, J. Chem. 2013 (2013) 1–6, https://doi.org/10.1155/2013/250760.
[111] M. Jiang, X. Yu, H. Yang, S. Chen, Optimization strategies of preparation of biomass-derived carbon electrocatalyst for boosting oxygen reduction reaction: a minireview, Catalysts 10 (2020) 1–17, https://doi.org/10.3390/catal10121472.
[112] X. Liu, Y. Zhou, W. Zhou, L. Li, S. Huang, S. Chen, Biomass-derived nitrogen self-doped porous carbon as effective metal-free catalysts for oxygen reduction reaction, Nanoscale 7 (2015) 6136–6142, https://doi.org/10.1039/c5nr00013k.
[113] Y. Sun, Y. Ouyang, J. Luo, H. Cao, X. Li, J. Ma, J. Liu, Y. Wang, L. Lu, Biomass-derived nitrogen self-doped porous activation carbon as an effective bifunctional electrocatalysts, Chinese Chem. Lett. 32 (2021) 92–98, https://doi.org/10.1016/j.cclet.2020.09.027.
[114] L. Xu, H. Fan, L. Huang, J. Xia, S. Li, M. Li, H. Ding, K. Huang, Chrysanthemum-derived N and S co-doped porous carbon for efficient oxygen reduction reaction and aluminum-air battery, Electrochim. Acta 239 (2017) 1–9, https://doi.org/10.1016/j.electacta.2017.04.002.
[115] P. Vengatesh, C. Karthik Kumar, T.S. Shyju, M. Paulraj, Biomass-derived carbon as electrode materials for batteries, in: Biomass-Derived Carbon Mater. Prod, Appl., Wiley, 2022, pp. 171–213, https://doi.org/10.1002/9783527832903.ch8.
[116] Y. Sun, X.L. Shi, Y.L. Yang, G. Suo, L. Zhang, S. Lu, Z.G. Chen, Biomass-derived carbon for high-performance batteries: from structure to properties, Adv. Funct. Mater. 32 (2022) 2201584, https://doi.org/10.1002/adfm.202201584.
[117] A. Beda, J.M. Le Meins, P.L. Taberna, P. Simon, C. Matei Ghimbeu, Impact of biomass inorganic impurities on hard carbon properties and performance in Na-ion batteries, Sustain. Mater. Technol. 26 (2020) 1–41, https://doi.org/10.1016/j.susmat.2020.e00227.
[118] R. Boonprachai, T. Autthawong, O. Namsar, C. Yodbunork, W. Yodying, T. Sarakonsri, Natural porous carbon derived from popped rice as anode materials for lithium-ion batteries, Crystals 12 (2022) 1–15, https://doi.org/10.3390/cryst12020223.
[119] S. Mateti, I. Sultana, Y. Chen, M. Kota, M.M. Rahman, Boron nitride-based nanomaterials: synthesis and application in rechargeable batteries, Batteries 9 (2023) 344, https://doi.org/10.3390/batteries9070344.
[120] J. Min, X. Wen, T. Tang, X. Chen, K. Huo, J. Gong, J. Azadmanjiri, C. He, E. Mijowska, A general approach towards carbonization of plastic waste into a well-designed 3D porous carbon framework for super lithium-ion batteries, Chem. Commun. 56 (2020) 9142–9145, https://doi.org/10.1039/d0cc03236k.
[121] C. Hernández-Rentero, V. Marangon, M. Olivares-Marín, V. Gómez-Serrano, Á. Caballero, J. Morales, J. Hassoun, Alternative lithium-ion battery using biomass-derived carbons as environmentally sustainable anode, J. Colloid Interface Sci. 573 (2020) 396–408, https://doi.org/10.1016/j.jcis.2020.03.092.
[122] Y. Qiao, H. Yang, Z. Chang, H. Deng, X. Li, H. Zhou, A high-energy-density and long-life initial-anode-free lithium battery enabled by a Li2O sacrificial agent, Nat. Energy 6 (2021) 653–662, https://doi.org/10.1038/s41560-021-00839-0.
[123] P. Molaiyan, G.S. Dos Reis, D. Karuppiah, C.M. Subramaniyam, F. García-Alvarado, U. Lassi, Recent progress in biomass-derived carbon materials for Li-ion and Na-ion batteries—a review, Batteries 9 (2023) 116, https://doi.org/10.3390/batteries9020116.
[124] S. Mopoung, R. Sitthikhankaew, N. Mingmoon, Preparation of anode material for lithium battery from activated carbon, Int. J. Renew. Energy Dev. 10 (2021) 91–96, https://doi.org/10.14710/ijred.2021.32997.
[125] J.H. Um, Y. Kim, C.Y. Ahn, J. Kim, Y.E. Sung, Y.H. Cho, S.S. Kim, W.S. Yoon, Biomass waste, coffee grounds-derived carbon for lithium storage, J. Electrochem. Sci. Technol. 9 (2018) 163–168, https://doi.org/10.5229/JECST.2018.9.3.163.
[126] E. Hastuti, A. Subhan, D. Puspitasari, Synthesis of activated carbon derived from chicken feather for Li-ion batteries through chemical and physical activation process, Mater. Renew. Sustain. Energy. 10 (2021) 1–9, https://doi.org/10.1007/s40243-021-00198-6.
[127] S. Wong, N. Ngadi, I.M. Inuwa, O. Hassan, Recent advances in applications of activated carbon from biowaste for wastewater treatment: a short review, J. Clean. Prod. 175 (2018) 361–375, https://doi.org/10.1016/j.jclepro.2017.12.059.
[128] Z. Guan, Z. Guan, Z. Li, J. Liu, K. Yu, Characterization and preparation of nano-porous carbon derived from hemp stems as anode for lithium-ion batteries, Nanoscale Res. Lett. 14 (2019) 1–9, https://doi.org/10.1186/s11671-019-3161-1.
[129] X. Yu, K. Zhang, N. Tian, A. Qin, L. Liao, R. Du, C. Wei, Biomass carbon derived from sisal fiber as anode material for lithium-ion batteries, Mater. Lett. 142 (2015) 193–196, https://doi.org/10.1016/j.matlet.2014.11.160.
[130] S. Duan, X. Wu, K. Zeng, T. Tao, Z. Huang, M. Fang, Y. Liu, X. Min, Simple routes from natural graphite to graphite foams: preparation, structure and properties, Carbon N. Y. 159 (2020) 527–541, https://doi.org/10.1016/j.carbon.2019.12.091.
[131] J.H. Kim, E. Jeong, Y.S. Lee, Preparation and characterization of graphite foams, J. Ind. Eng. Chem. 32 (2015) 21–33, https://doi.org/10.1016/j.jiec.2015.09.003.
[132] M. Muraleedharan Pillai, N. Kalidas, X. Zhao, V.P. Lehto, Biomass-based silicon and carbon for lithium-ion battery anodes, Front. Chem. 10 (2022) 1–11, https://doi.org/10.3389/fchem.2022.882081.
[133] B.P. Thapaliya, H. Luo, P. Halstenberg, H.M. Meyer, J.R. Dunlap, S. Dai, Low-cost transformation of biomass-derived carbon to high-performing nano-graphite via low-temperature electrochemical graphitization, ACS Appl. Mater. Interfaces 13 (2021) 4393–4401, https://doi.org/10.1021/acsami.0c19395.
[134] T.J. Yokokura, J.R. Rodriguez, V.G. Pol, Waste biomass-derived carbon anode for enhanced lithium storage, ACS Omega 5 (2020) 19715–19720, https://doi.org/10.1021/acsomega.0c02389.
[135] K. Yu, J. Li, H. Qi, C. Liang, High-capacity activated carbon anode material for lithium-ion batteries prepared from rice husk by a facile method, Diam. Relat. Mater. 86 (2018) 139–145, https://doi.org/10.1016/j.diamond.2018.04.019.
[136] J.Y. Hwang, S.T. Myung, Y.K. Sun, Sodium-ion batteries: present and future, Chem. Soc. Rev. 46 (2017) 3529–3614, https://doi.org/10.1039/c6cs00776g.

[137] A. Benítez, J. Amaro-Gahete, Y.C. Chien, Á. Caballero, J. Morales, D. Brandell, Recent advances in lithium-sulfur batteries using biomass-derived carbons as sulfur host, Renew. Sustain. Energy Rev. 154 (2022), https://doi.org/10.1016/j.rser.2021.111783.
[138] Z. Gao, Y. Zhang, N. Song, X. Li, Biomass-derived renewable carbon materials for electrochemical energy storage, Mater. Res. Lett. 5 (2017) 69–88, https://doi.org/10.1080/21663831.2016.1250834.
[139] M. Liu, Y. Chen, K. Chen, N. Zhang, X. Zhao, F. Zhao, Z. Dou, X. He, L. Wang, Biomass-derived activated carbon for rechargeable lithium-sulfur batteries, Bioresources 10 (2015) 155–168, https://doi.org/10.15376/biores.10.1.155-168.
[140] S.B. Ma, D.J. Lee, V. Roev, D. Im, S.G. Doo, Effect of porosity on electrochemical properties of carbon materials as cathode for lithium-oxygen battery, J. Power Sources 244 (2013) 494–498, https://doi.org/10.1016/j.jpowsour.2013.03.150.
[141] C. Fan, R. Yang, Y. Huang, Y. Yan, Y.Y. Yang, Y. Yang, Y. Zou, Y. Xu, Hierarchical multi-channels conductive framework constructed with rGO modified natural biochar for high sulfur areal loading self-supporting cathode of lithium-sulfur batteries, Chem. Eng. J. Adv. 9 (2022) 100209, https://doi.org/10.1016/j.ceja.2021.100209.
[142] Y. Dessie, S. Tadesse, R. Eswaramoorthy, Surface roughness and electrochemical performance properties of biosynthesized α -MnO2/NiO-based polyaniline ternary composites as efficient catalysts in microbial fuel cells, J. Nanomater. 2021 (2021) 1–21, https://doi.org/10.1155/2021/7475902.
[143] D. Li, Z. Han, K. Leng, S. Ma, Y. Wang, J. Bai, Biomass wood-derived efficient Fe–N–C catalysts for oxygen reduction reaction, J. Mater. Sci. 56 (2021) 12764–12774, https://doi.org/10.1007/s10853-021-06122-7.
[144] A. Iqbal, O.M. El-Kadri, N.M. Hamdan, Insights into rechargeable Zn-air batteries for future advancements in energy storing technology, J. Energy Storage 62 (2023) 106926, https://doi.org/10.1016/j.est.2023.106926.
[145] D. Deckenbach, J.J. Schneider, A long-overlooked pitfall in rechargeable zinc–air batteries: proper electrode balancing, Adv. Mater. Interfaces. 10 (2023) 1765–1780, https://doi.org/10.1002/admi.202202494.
[146] S. Pakseresht, M. Celik, A. Guler, A.W.M. Al-Ogaili, T. Kallio, Recent advances in all-solid-state lithium–oxygen batteries: challenges, strategies, Future, Batteries. 9 (2023) 380, https://doi.org/10.3390/batteries9070380.
[147] A. Arjunan, M. Subbiah, M. Sekar, V.S. Ajay Piriya, V. Balasubramanian, R. Sundara, Biomass derived hierarchically porous carbon inherent structure as an effective metal free cathode for Li-O2/air battery, Electrochem. Sci. Adv. 1 (2021) 1–13, https://doi.org/10.1002/elsa.202000037.
[148] T. Zhao, Y. Yao, Y. Yuan, M. Wang, F. Wu, K. Amine, J. Lu, A universal method to fabricating porous carbon for Li-O2 battery, Nano Energy 82 (2021), https://doi.org/10.1016/j.nanoen.2021.105782.
[149] F. Ahmed, G. Almutairi, P.M.Z. Hasan, S. Rehman, S. Kumar, N.M. Shaalan, A. Aljaafari, A. Alshoaibi, B. AlOtaibi, K. Khan, Fabrication of a biomass-derived activated carbon-based anode for high-performance Li-ion batteries, Micromachines 14 (2023) 192, https://doi.org/10.3390/mi14010192.
[150] N. Issatayev, G. Kalimuldina, A. Nurpeissova, Z. Bakenov, Biomass-derived porous carbon from agar as an anode material for lithium-ion batteries, Nanomaterials 12 (2022) 22, https://doi.org/10.3390/nano12010022.
[151] H. Wan, X. Hu, From biomass-derived wastes (bagasse, wheat straw and shavings) to activated carbon with three-dimensional connected architecture and porous structure for Li-ion batteries, Chem. Phys. 521 (2019) 108–114, https://doi.org/10.1016/j.chemphys.2019.01.012.
[152] J. Hao, Y. Wang, C. Chi, J. Wang, Q. Guo, Y. Yang, Y. Li, X. Liu, J. Zhao, Enhanced storage capability by biomass-derived porous carbon for lithium-ion and sodium-ion battery anodes, Sustain. Energy Fuels 2 (2018) 2358–2365, https://doi.org/10.1039/c8se00353j.
[153] T.K. Kumaresan, S.A. Masilamani, K. Raman, S.Z. Karazhanov, R. Subashchandrabose, High performance sodium-ion battery anode using biomass derived hard carbon with engineered defective sites, Electrochim. Acta 368 (2021) 137574, https://doi.org/10.1016/j.electacta.2020.137574.
[154] Y. Feng, L. Tao, Y. He, Q. Jin, C. Kuai, Y. Zheng, M. Li, Q. Hou, Z. Zheng, F. Lin, H. Huang, Chemical-enzymatic fractionation to unlock the potential of biomass-derived carbon materials for sodium ion batteries, J. Mater. Chem. A. 7 (2019) 26954–26965, https://doi.org/10.1039/c9ta09124f.
[155] S. Jo, J.W. Hong, T. Momma, Y. Park, J. Heo, J.W. Park, S. Ahn, Facile one-pot synthesis of biomass-derived activated carbon as an interlayer material for a BAC/PE/Al2O3 dual coated separator in Li-S batteries, RSC Adv. 13 (2023) 27274–27282, https://doi.org/10.1039/d3ra05891c.
[156] H. Chen, P. Xia, W. Lei, Y. Pan, Y. Zou, Z. Ma, Preparation of activated carbon derived from biomass and its application in lithium–sulfur batteries, J. Porous Mater. 26 (2019) 1325–1333, https://doi.org/10.1007/s10934-019-00720-2.
[157] J. Zhang, J. Xiang, Z. Dong, Y. Liu, Y. Wu, C. Xu, G. Du, Biomass derived activated carbon with 3D connected architecture for rechargeable lithium - sulfur batteries, Electrochim. Acta 116 (2014) 146–151, https://doi.org/10.1016/j.electacta.2013.11.035.
[158] M. Wang, J. Ma, H. Yang, G. Lu, S. Yang, Z. Chang, Nitrogen and cobalt Co-coped carbon materials derived from biomass chitin as high-performance electrocatalyst for aluminum-air batteries, Catalysts 9 (2019) 954, https://doi.org/10.3390/catal9110954.
[159] J. Feng, R. Tang, X. Wang, T. Meng, Biomass-derived activated carbon sheets with tunable oxygen functional groups and pore volume for high-performance oxygen reduction and Zn-air batteries, ACS Appl. Energy Mater. 4 (2021) 5230–5236, https://doi.org/10.1021/acsaem.1c00755.
[160] M. Wang, Y. Yao, Z. Tang, T. Zhao, F. Wu, Y. Yang, Q. Huang, Self-nitrogen-doped carbon from plant waste as an oxygen electrode material with exceptional capacity and cycling stability for lithium-oxygen batteries, ACS Appl. Mater. Interfaces 10 (2018) 32212–32219, https://doi.org/10.1021/acsami.8b11282.
[161] M. Zhang, J. Zhang, S. Ran, W. Sun, Z. Zhu, Biomass-Derived sustainable carbon materials in energy conversion and storage applications: status and opportunities. A mini review, Electrochem. Commun. 138 (2022) 107283, https://doi.org/10.1016/j.elecom.2022.107283.
[162] L. Yan, J. Yu, J. Houston, N. Flores, H. Luo, Biomass derived porous nitrogen doped carbon for electrochemical devices, Green Energy Environ. 2 (2017) 84–99, https://doi.org/10.1016/j.gee.2017.03.002.